

A fluorine scan of the phenylamidinium needle of tricyclic thrombin inhibitors: effects of fluorine substitution on pK_a and binding affinity and evidence for intermolecular C–F \cdots CN interactions

Jacob Olsen,^a Paul Seiler,^a Björn Wagner,^b Holger Fischer,^b Thomas Tschopp,^b Ulrike Obst-Sander,^b David W. Banner,^b Manfred Kansy,^b Klaus Müller^b and François Diederich^{*a}

^a *Laboratorium für Organische Chemie, ETH-Hönggerberg, HCI, CH-8093 Zürich, Switzerland. E-mail: diderich@org.chem.ethz.ch*

^b *Pharma Division, Präklinische Forschung, F. Hoffmann-La Roche AG, CH-4002 Basel, Switzerland*

Received 19th February 2004, Accepted 18th March 2004
First published as an Advance Article on the web 14th April 2004

The H-atoms of the phenylamidinium needle of tricyclic thrombin inhibitors, which interacts with Asp189 at the bottom of the selectivity pocket S1 of the enzyme, were systematically exchanged with F-atoms in an attempt to improve the pharmacokinetic properties by lowering the pK_a value. Both the pK_a values and the inhibitory constants K_i against thrombin and trypsin were decreased upon F-substitution. Interestingly, linear free energy relationships (LFERs) revealed that binding affinity against thrombin is much more affected by a decrease in pK_a than the affinity against trypsin. Surprising effects of F-substitutions in the phenylamidinium needle on the pK_a value of the tertiary amine centre in the tricyclic scaffold of the inhibitors were observed and subsequently rationalised by X-ray crystallographic analysis and *ab initio* calculations. Evidence for highly directional intermolecular C–F \cdots CN interactions was obtained by analysis of small-molecule X-ray crystal structures and investigations in the Cambridge Structural Database (CSD).

Introduction

The importance of organofluorine in medicinal chemistry has been increasing ever since the seminal discovery in 1954 by Fried and Sabo that introduction of a single F-atom in the 9 α -position of cortisone acetate led to an increase in biological activity by a factor of 7–10.^{1,2} This historical case illustrates well the complexity of the factors that may account for favourable/unfavourable effects of F-substitution. Initially, the enhanced biological activity of 9 α -fluorocorticosteroids was ascribed to an enhanced polarisation of the neighbouring 11 β -OH group by the strongly electron-withdrawing F-atom. Later, it was attributed to conformational changes in the steroidal A-ring induced by the F-substituent (van der Waals radius: 1.47 Å) that is slightly larger than a H-substituent (1.20 Å).^{3,4} Even after the crystal structure analysis revealed the binding mode of 9 α -fluorocortisol, complexed to the ligand-binding domain of a mutant human androgen receptor,⁵ a good explanation of the positive effect of 9 α -F-substitution on biological activity remained elusive. Most F-effects on protein–ligand binding affinity/selectivity have indeed been discovered on a trial-and-error basis.² In contrast, modulation of the physico-chemical properties (such as lipophilicity, metabolic stability, acid/base properties) of drug candidates by introduction of F-substituents is more predictable.⁶

We have initiated a program to increase the knowledge of how the thermodynamics of protein–ligand interactions are affected by H- to F-mutations. In an experimental fluorine scan, we undertook a systematic exchange of H- for F-substituents in a rigid tricyclic thrombin inhibitor developed by *de novo* design.⁷ With a conserved binding mode of the ligands in the active site of thrombin, we hoped to obtain valuable structure–activity relationships (SARs), thereby making thermodynamic F-effects more predictable and helping to improve computational algorithms for predicting them.⁸ Thus, we recently

reported the F-scan of the benzyl substituent in the tricyclic thrombin inhibitors, pointing into the hydrophobic D-pocket (Fig. 1).⁹ A single H/F mutation in position 4 of the benzylic substituent in **1** resulted in a favourable F-interaction with the H–C α –C=O moiety of Asn98 lining the D-pocket and was found to increase the binding free enthalpy by $\Delta(\Delta G) \approx 1$ kcal

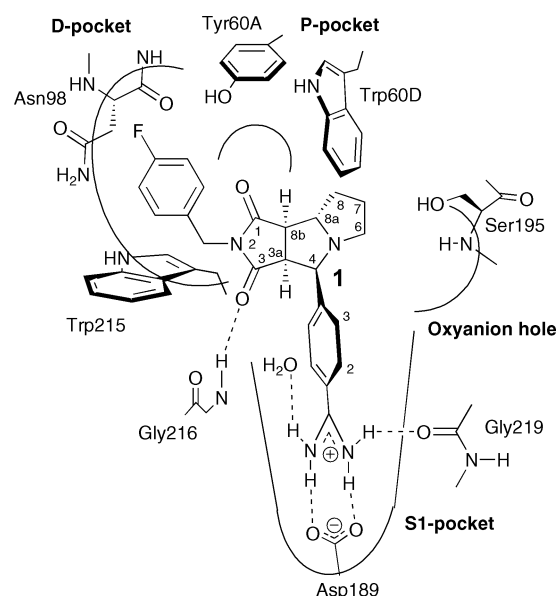


Fig. 1 Schematic representation of the binding mode of the tricyclic inhibitor **1** in the active site of thrombin. Only the (3*a*,*S*,4*R*,8*a*,*S*,8*b**R*)-configured enantiomer is bound, according to X-ray crystallography.^{7*a*,*b*,*9*} In addition to the catalytic triad flanked by the oxyanion hole, the active site is described in terms of the selectivity pocket S1, a small hydrophobic proximal pocket P and a large hydrophobic pocket D.

mol⁻¹. This study revealed that peptidic H-C_α-C=O fragments provide a pronounced fluorophilic environment. Previously unrecognised favorable C-F...C=O contacts are best described in terms of multipolar interactions between the intrinsically polar C-F and C=O units. Database mining showed that, as the F-atom approaches the carbonyl C-atom, it is preferentially located at or near the pseudo-trigonal axis of the carbonyl system.

Here, we report a fluorine scan on the phenylamidinium side chain (the so-called “needle”) of the tricyclic thrombin inhibitors bound in the narrow selectivity pocket S1. A large number of thrombin inhibitors feature as a crucial recognition element such a needle that is a surrogate of the Arg side chain in the natural substrate.¹⁰ Benzamidinium itself is an inhibitor of thrombin (inhibitory constant $K_i = 320 \mu\text{M}$) and the related serine protease trypsin ($K_i = 20 \mu\text{M}$).^{11,12} It binds into the S1-pockets of the two enzymes, that differ only by one amino acid, Ser190 in thrombin and Ala190 in trypsin. The phenylamidinium needle of **1** adopts a similar geometry in the S1-pocket of thrombin, forming a bidentate salt bridge with Asp189 (Figs. 1 and 2). Its high basicity ($\text{p}K_a$ of benzamidinium = 11.41^{12c}) prevents good oral bioavailability. One approach to overcome this problem could be a lowering of the basicity,¹³ and this could possibly be achieved by fluorination of the needle. To the best of our knowledge, the modulation of the phenylamidinium $\text{p}K_a$ through systematic F-substitution has not been previously described, although mono-substitution of H with F has recently been reported.¹⁴

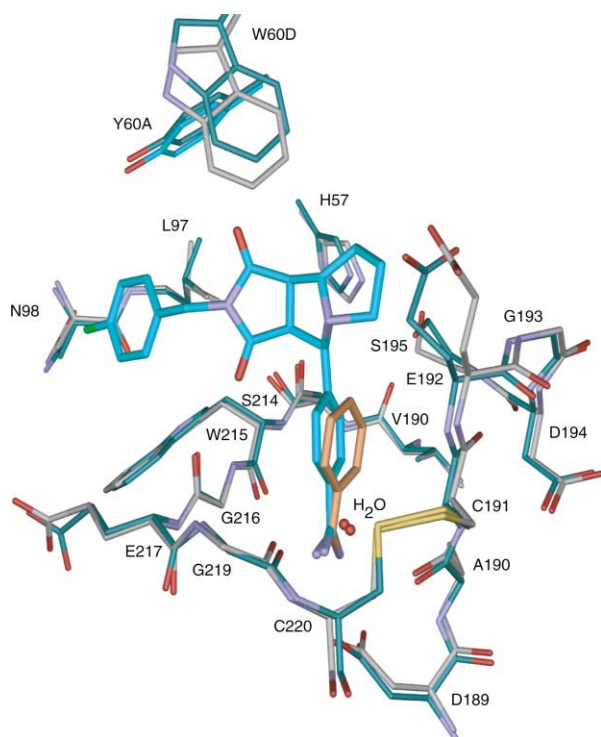


Fig. 2 Overlay of the crystal structures of **1** (protein data bank (pdb) code: 1OYT) and benzamidinium (1C5O) bound in the active site of thrombin. Color code: C-skeletons of protein and ligand in the complex of **1**: cyan; C-skeleton of benzamidinium: golden; C-skeleton of thrombin in the benzamidinium complex: grey; O-atoms: red, S-atoms: yellow, N-atoms: blue.

In this paper, we analyse how F-substitution of the phenylamidinium needle in the tricyclic thrombin inhibitors affects the $\text{p}K_a$ of this binding element and the inhibitory constants K_i against thrombin and trypsin. QSAR (quantitative structure-activity relationship) analysis of 3- and 4-substituted benzamidinium ligands has previously revealed a significant negative correlation between the binding affinity to both enzymes and the Hammett substituent σ : electron-withdrawing

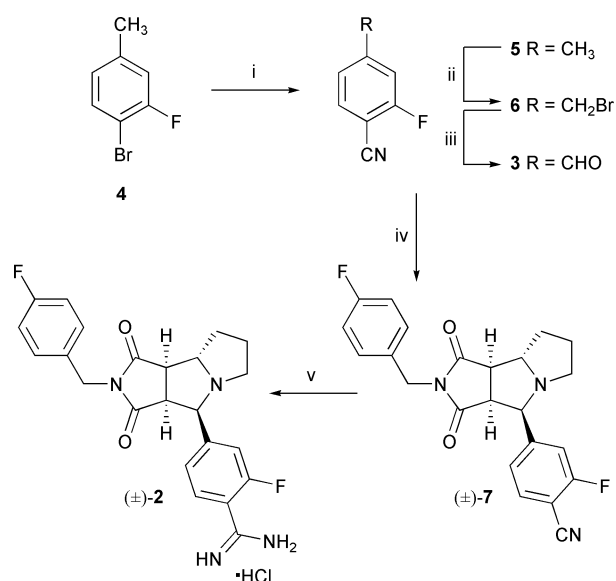
substituents decrease the binding affinity.^{11,12} Monte-Carlo simulations in conjunction with free-energy perturbation calculations by Jorgensen and co-workers nicely reproduced some of the relative experimental binding free energies.¹⁵ According to these calculations, different affinities are best rationalised by bulk solvation effects while other computational studies also invoke differences in the interactions with the protein environment.¹⁶ Isothermal calorimetric studies revealed that the binding of 4-substituted benzamidinium ligands to trypsin at room temperature is driven by a large favorable enthalpic term and a small favorable entropic term; however, as a result of a large negative change in heat capacity, the net thermodynamic driving force is highly temperature-dependent.¹¹

The work presented herein contributes to the foundation of the design of thrombin-selective inhibitors and resolves the complexity of some of the effects of fluorine substitution on protein binding affinity and selectivity, on physical properties such as $\text{p}K_a$ and $\log D$ and on molecular conformation.

Results and discussion

Synthesis

The construction of the tricyclic skeleton of the 2-fluorinated (*ortho* to the amidinium residue) inhibitor (\pm)-**2** required the preparation of 2-fluoro-4-formylbenzonitrile (**3**) (Scheme 1). Br \rightarrow CN exchange transformed commercial bromide **4** into the benzonitrile **5** which was brominated (NBS) to give the benzyl bromide **6**.¹⁷ Finally, **3** was obtained by oxidation of **6** with TMAO (trimethylamine-*N*-oxide).¹⁸



Scheme 1 Synthesis of inhibitor (\pm)-**2**. Reagents and conditions: i, CuCN, DMF, Δ ; quant.; ii, NBS, AIBN, CCl_4 , Δ ; 55%; iii, TMAO-2 H_2O , Me_2SO , CH_2Cl_2 , 0 °C; 74%; iv, *N*-(4-fluorobenzyl)maleimide, L-proline, MeCN, Δ ; 14%; v, AcCl, MeOH, CH_2Cl_2 , 5 °C; then NH_3 , MeOH, 65 °C; 56%. NBS = *N*-bromosuccinimide; AIBN = azobisisobutyronitrile; TMAO = trimethylamine *N*-oxide.

1,3-Dipolar cycloaddition^{7,19} of **3**, L-proline and *N*-(4-fluorobenzyl)maleimide^{9b} gave a mixture of diastereoisomers that was separated by column chromatography to afford the desired benzonitrile (\pm)-**7**. The configuration of the tricyclic skeleton was initially assigned by ¹H NMR and NOESY spectroscopy and later confirmed by X-ray crystallography (Fig. 3). Finally, Pinner reaction provided inhibitor (\pm)-**2**.

For the synthesis of inhibitor (\pm)-**8** with the F-substituent in position 3 of the phenylamidinium needle, 3-fluoro-4-formylbenzonitrile (**9**) was prepared from **10** by benzylic bromination (\rightarrow **11**) and oxidation, as described for **3** (Scheme 2).²⁰ 1,3-Dipolar cycloaddition followed by column chromatography

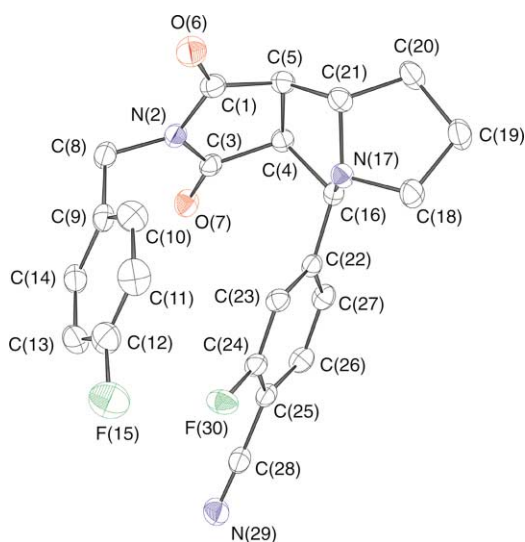
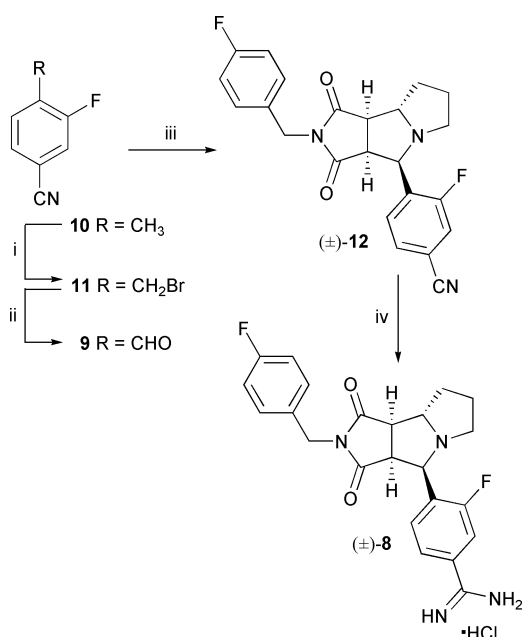


Fig. 3 ORTEP representation of (\pm)-**7** with vibrational ellipsoids obtained at 223 K and shown at the 30% probability level.



Scheme 2 Synthesis of inhibitor (\pm)-**8**. *Reagents and conditions:* i, NBS, AIBN, CCl_4 , Δ ; 61%; ii, TMAO-2 H_2O , Me_2SO , CH_2Cl_2 , 0 °C; 73%; iv, *N*-(4-fluorobenzyl)maleimide, L-proline, MeCN, Δ ; 22%; v, AcCl, MeOH, CH_2Cl_2 , 5 °C; then NH_3 , MeOH, 65 °C; 79%.

provided nitrile (\pm)-**12**, and its configuration was proven by X-ray crystallography (Fig. 4). Subsequent Pinner reaction yielded inhibitor (\pm)-**8**.

The difluorinated benzonitriles **13–15** for the synthesis of inhibitors (\pm)-**16**–(\pm)-**18**, respectively, (Scheme 3) could be effectively prepared from commercially available difluorinated starting materials (**19–21**) by utilising fluorine-directed *ortho*-metallation as the key transformation.²¹ Compound **13** was obtained in high yield by *ortho*-lithiation of **19** with LDA at -78 °C, followed by quenching with DMF. 1,3-Dipolar cycloaddition provided (\pm)-**22**, and its configuration was proven by X-ray crystallography (Fig. 5).

ortho-Lithiated **20** was highly unstable even at -78 °C and decomposed rapidly to an unidentified polar by-product (TLC). Quenching with DMF immediately after lithiation afforded benzonitrile **14** that was converted *via* (\pm)-**23** into inhibitor (\pm)-**17**.

For the synthesis of (\pm)-**18**, aldehyde **21** was transformed into 1,3-dioxolane **24** that was *ortho*-lithiated and transformed with tosyl cyanide²² into nitrile **25** and finally, by deprotection,

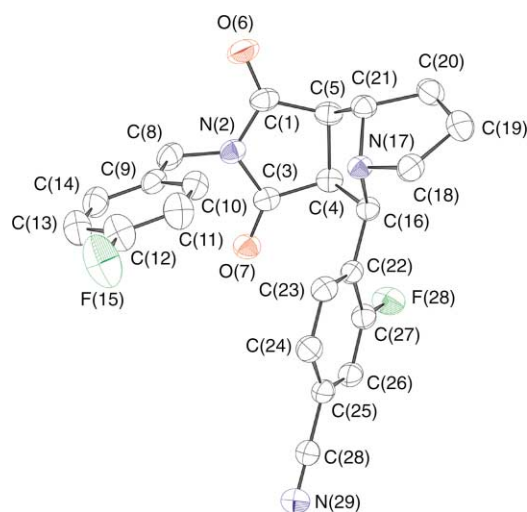


Fig. 4 ORTEP representation of (\pm)-**12** with vibrational ellipsoids obtained at 223 K and shown at the 30% probability level.

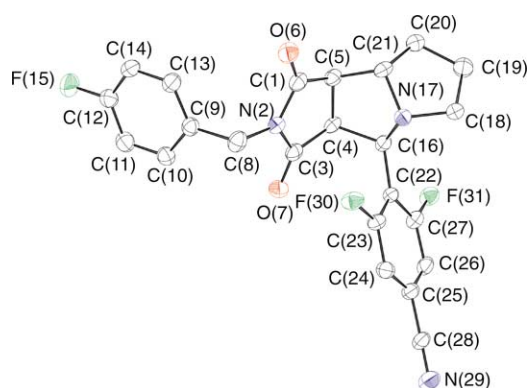


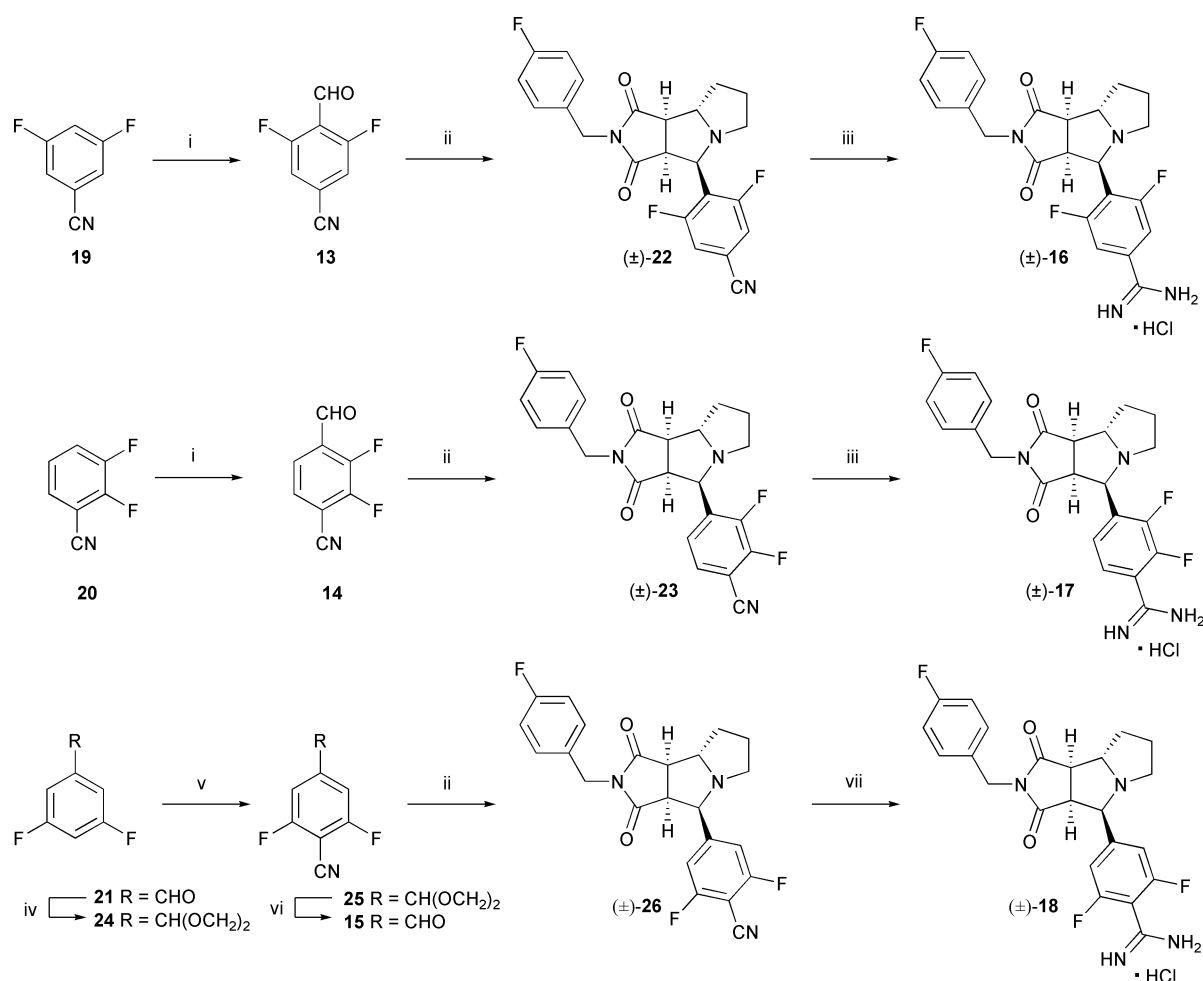
Fig. 5 ORTEP representation of (\pm)-**22** with vibrational ellipsoids obtained at 243 K and shown at the 30% probability level.

into 4-formylbenzonitrile **15**. 1,3-Dipolar cycloaddition afforded an unusually complex mixture of diastereoisomers, and the desired tricyclic product (\pm)-**26** was only obtained after tedious column chromatography. Attempts to convert (\pm)-**26** into inhibitor (\pm)-**18** by the Pinner reaction failed and gave only starting material, even after one week. This transformation is clearly sensitive to the presence of two substituents *ortho* to the CN group. Instead, the desired conversion of (\pm)-**26** into (\pm)-**18** was possible by reaction with hydroxylamine, acetylation and hydrogenation over Pd/C.²³

Small molecule crystal packing analysis

The crystal packings of the solved small molecule structures were analysed^{24–26} to obtain additional information on the preferred environment for the small, hard and strongly electro-negative F-substituents and for gaining further insight into non-covalent interactions involving C–F residues. Such analysis had previously been extremely useful in establishing weak C–F \cdots H–C $_{\alpha}$ –C=O and C–F \cdots C=O interactions.⁹

Close C–F \cdots H–C contacts. Several investigations on the H-bonding potential of organic C–F residues have appeared.²⁵ Whereas the F^- anion is the strongest known H-bond acceptor, it has become clear from crystallographic and computational studies that organic C–F is a considerably weaker H-bond acceptor than C–N or C–O groups. Thus, Dunitz and Taylor found only very few cases in the Cambridge Structural Database (CSD) of what, by geometrical considerations, could be classified as moderate H-bonds with C–F as the acceptor.^{25a} Whether short contacts between C–F residues and strong H-bond donors such as O–H, reported in the literature,²⁷ are true H-bonds or should rather be seen as multipolar inter-



Scheme 3 Synthesis of inhibitors (±)-16–(±)-18. *Reagents and conditions:* i, LDA, THF, hexane, $-78\text{ }^{\circ}\text{C}$; then DMF; 82% (**13**), 35% (**14**); ii, *N*-(4-fluorobenzyl) maleimide, L-proline, MeCN, Δ ; 29% ((±)-**22**), 37% ((±)-**23**), 15% ((±)-**26**); iii, AcCl, MeOH, CH_2Cl_2 , $5\text{ }^{\circ}\text{C}$; then NH_3 , MeOH, $65\text{ }^{\circ}\text{C}$; 58% ((±)-**16**), 43% ((±)-**17**); iv, $\text{HOCH}_2\text{CH}_2\text{OH}$, $\text{TsOH}\cdot\text{H}_2\text{O}$, Δ ; v) LDA, THF, hexane, $-78\text{ }^{\circ}\text{C}$; then tosyl cyanide; vi, HCl, H_2O , THF, Δ ; 48% (over 3 steps); vii, NH_2OH , MeOH, THF, then Ac_2O , then H_2 , Pd/C; 39%. LDA = lithium diisopropylamide; DMF = dimethylformamide, THF = tetrahydrofuran.

actions remains a matter of ongoing discussion. This is even more true for the increasing number of C–H \cdots F–C interactions,^{9,28} involving very weak H-bond donors, that are observed in crystal structures. Independent of naming and classification, these contacts could make small yet selective energetic contributions to protein–ligand binding.

For the packing analysis described in the following, idealised C–H distances of 1.08 Å were used. In the crystal packing of nitrile (±)-**7** (see Fig. 3), the shortest intermolecular contact of the two F-atoms is between F(30) and the *exo* H-atom of C(20) (distance $d(\text{F} \cdots \text{H}-\text{C})$ 2.32 Å, $d(\text{F} \cdots \text{C})$ 3.34, angle $\alpha(\text{F} \cdots \text{H}-\text{C})$ 157°). An interesting intramolecular contact is seen in which the F(30)-atom of the benzonitrile moiety is situated on top of the electrophilic C(12)-atom of the benzyl C–F group ($d(\text{F} \cdots \text{C}-\text{F})$ 3.09 Å. This C–F \cdots C–F interaction bears resemblance to the C–F \cdots C=O dipolar interaction.⁹

The crystal packing of (±)-**12** (Fig. 6) features an extraordinarily short intermolecular contact between F(15) of the benzyl group and the polarised C(24)–H *ortho* to the CN group ($d(\text{F} \cdots \text{H}-\text{C})$ 2.22 Å, $d(\text{F} \cdots \text{C})$ 3.04 Å, $\alpha(\text{F} \cdots \text{H}-\text{C})$ 131°). This F \cdots H distance is significantly shorter than the sum of the van der Waals radii (2.67 Å) and represents the shortest $\text{C}_{\text{aryl}}-\text{F} \cdots \text{H}-\text{C}_{\text{aryl}}$ contact observed in small molecule crystal structures.^{28,29} C–F \cdots H–C contacts have not only been recognised in protein–ligand interactions³⁰ and in small molecule crystal packings^{9,28} but have also been implied in catalytic processes.^{29,31} The second polarised C(26)–H, *ortho* to both CN- and F-substituents, contacts the imide carbonyl O(7)

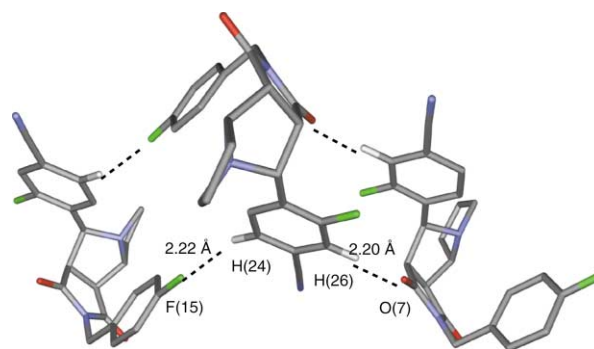


Fig. 6 Short intermolecular $\text{C}_{\text{aryl}}-\text{F} \cdots \text{H}-\text{C}_{\text{aryl}}$ contact observed in the crystal packing of (±)-**12**.

($d(\text{O} \cdots \text{H}-\text{C})$ 2.19 Å, $d(\text{O} \cdots \text{C})$ 3.25 Å, $\alpha(\text{O} \cdots \text{H}-\text{C})$ 165°), thereby presenting another example for the weak, well-studied $\text{O} \cdots \text{H}-\text{C}$ hydrogen bond.^{26,32}

Close C–F \cdots CN contacts. Intramolecular C–F \cdots CN interactions have recently been reported.³³ In this investigation, we also observed several short *intermolecular* C–F \cdots CN contacts below the sum of the van der Waals radii (*ca.* 3.3 Å). Thus, in the crystal packing of difluorinated 4-formylbenzonitrile **13** (Fig. 7A), F(11) points directly toward the positively polarised C(9)-atoms of the cyano groups of two molecules in a neighboring stack ($d(\text{F} \cdots \text{CN})$ 3.11 Å, $d(\text{F} \cdots \text{NC})$ 3.36 Å, $\alpha(\text{F} \cdots \text{CN})$ 93° and $d(\text{F} \cdots \text{CN})$ 3.21 Å, $d(\text{F} \cdots \text{NC})$ 3.21 Å, $\alpha(\text{F} \cdots \text{CN})$ 80°). These polar C–F \cdots CN interactions

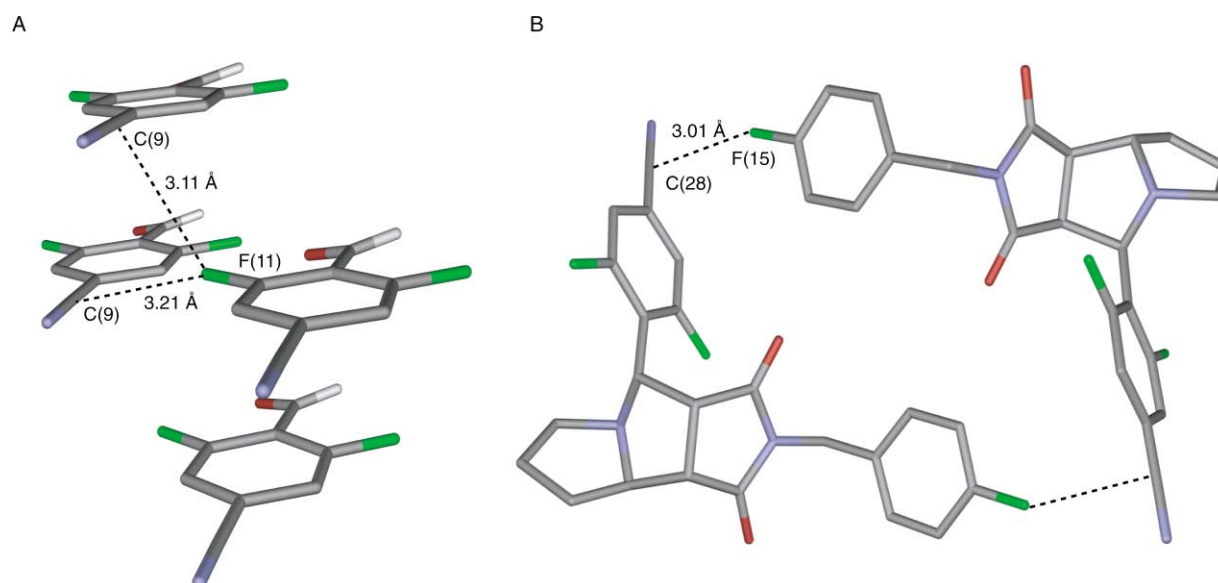


Fig. 7 Short intermolecular $C_{\text{aryl}}\text{-F} \cdots \text{CN}$ contacts observed in the crystal packings of **13** (A) and (\pm) -**22** (B).

probably stabilise the parallel-slipped stacks observed in the crystal structure. Also, in the crystal packing of (\pm) -**22**, a very short $\text{C-F} \cdots \text{CN}$ contact is found ($d(\text{F} \cdots \text{CN})$ 3.01 Å, $d(\text{F} \cdots \text{NC})$ 3.35 Å, $a(\text{F} \cdots \text{CN})$ 97°; Fig. 7B). These $\text{C-F} \cdots \text{CN}$ contacts bear strong resemblance to the multipolar $\text{C-F} \cdots \text{C=O}$ interactions we have previously described.⁹

These findings prompted us to search the CSD³⁴ for intermolecular interactions between C-F and CN moieties in crystals of fluorine-containing organic nitriles. The search resulted in 91 hits with a total of 261 occurrences of close $\text{F} \cdots \text{CN}$ contacts below 4.0 Å. There are quite a number of cases (44 occurrences, Fig. 8) with contact distances below the sum of the van der Waals radii (*ca.* 3.3 Å), indicating an attractive interaction between the two polar groups. An analysis of the relative orientation of the two interacting groups in terms of the non-bonded distance $d_1(\text{F} \cdots \text{CN})$ and the angles $a_1(\text{F} \cdots \text{CN})$ and $a_2(\text{C-F} \cdots \text{N})$ reveals that, at short contact distances, the F-atoms prefer a position perpendicular to the cyano group (Fig. 8). The C-F bond is generally inclined to the $\text{F} \cdots \text{C}$ axis with angles a_1 adopting values typically between 100°–170° at short contact distances. Thus, the results of the CSD search nicely parallel those of our previous investigations on $\text{C-F} \cdots \text{C=O}$ interactions.

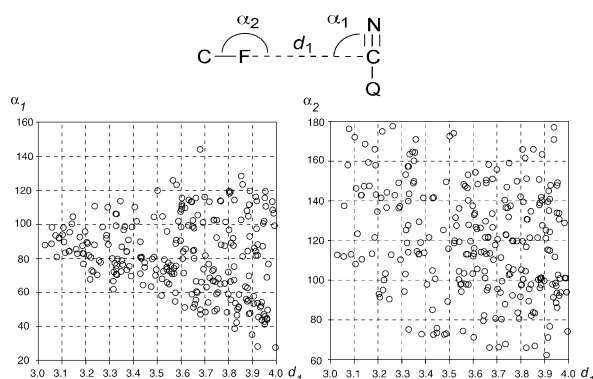


Fig. 8 Scatterplots of a_1 vs. d_1 (left) and a_2 vs. d_1 (right) of 261 occurrences of close $\text{C-F} \cdots \text{CN}$ contacts with $d_1 < 4.0$ Å obtained from 91 hits of the CSD search of fluorine-containing organic nitriles.

Influence of F-substitution on the $\text{p}K_a$ values of the inhibitors

The influence of F-substitution on the $\text{p}K_a$ values of the tertiary amino group in the tricyclic skeleton ($\text{p}K_{a1}$) and the amidinium residue ($\text{p}K_{a2}$) of the inhibitors was investigated (Table 1). Surprisingly, two different sets of $\text{p}K_a$ values were

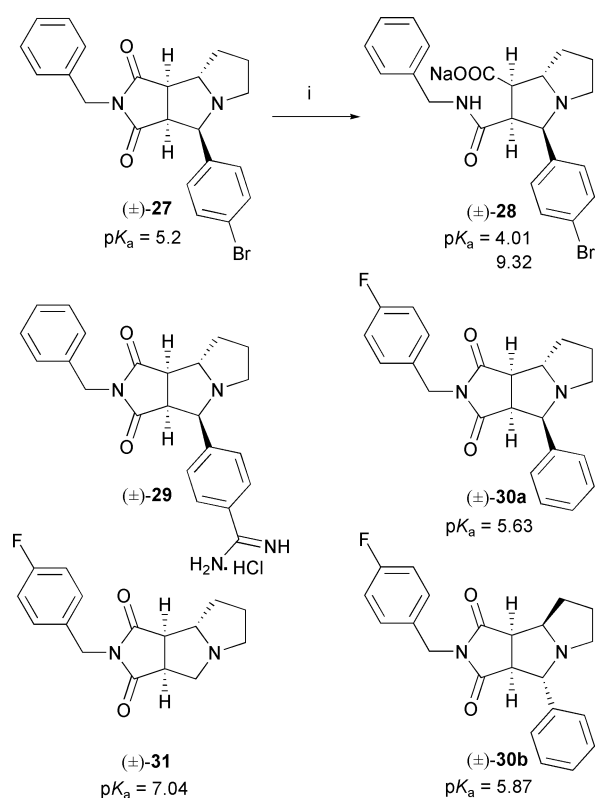
Table 1 Biological activities and physicochemical properties of the fluorinated tricyclic thrombin inhibitors

Inhibitor	K_i [μM] ^a	Selectivity ^b	$\text{p}K_{a1}$ ^c	$\text{p}K_{a2}$ ^c	$\log D$
(\pm) - 1	0.057	67	4.47	11.14	-1.16
(\pm) - 2	0.63	22	4.21	10.69	-1.08
(\pm) - 8	0.61	11	4.10	10.83	^d
(\pm) - 16	1.7	7.6	4.21	10.36	^d
(\pm) - 17	5.0	4.6	3.73	10.28	^d
(\pm) - 18	9.0	7.6	3.73	10.06	-0.35

^a The uncertainty of the measured K_i values is $\pm 20\%$. ^b $K_i(\text{trypsin})/K_i(\text{thrombin})$. ^c $\text{p}K_{a1}$: tertiary amine in tricyclic skeleton, $\text{p}K_{a2}$: phenylamidinium. Reproducibility of $\text{p}K_a$ values: ± 0.05 units. ^d Not determined.

measured for each compound, depending on whether the potentiometric titration was conducted from $\text{pH} \approx 2$ to $\text{pH} \approx 13$ or in the reverse way from $\text{pH} \approx 13$ to $\text{pH} \approx 2$. The effect was particularly pronounced for the tertiary amino group ($\text{p}K_{a1}$), yielding a higher apparent $\text{p}K_a$ value (by *ca.* 4 units) in the titration starting from basic solution. The effect on the $\text{p}K_a$ of the amidinium residue ($\text{p}K_{a2}$) was smaller, with a discrepancy of only *ca.* 0.2 units. Subsequent chemical analysis revealed that this discrepancy resulted from the instability of the inhibitors in basic solution and that the lower values included in Table 1, obtained by titrations starting from acidic solution, are the correct ones. In basic solution (0.05 M NaOH in THF/ H_2O 2 : 1), compounds such as (\pm) -**27**^{7d} undergo a surprisingly rapid, regioselective opening of the succinimide ring in the tricyclic skeleton to afford the corresponding sodium carboxylate (\pm) -**28**, as revealed by ^1H and ^{13}C NMR as well as high-resolution mass spectrometry (HR-MS) (Scheme 4). The proposed configuration of (\pm) -**28** was confirmed by a combination of 2D NMR sequences, including COSY (correlation spectroscopy), HSQC (heteronuclear single-quantum correlation) and HMBC (heteronuclear multiple bond correlation).³⁵ In (\pm) -**28**, the $\text{p}K_a$ value of the tertiary amine centre is raised by *ca.* 4 units, as compared to (\pm) -**27**. Base-induced ring opening in 0.05 M NaOD in D_2O was also confirmed by ^1H NMR spectroscopy for inhibitor (\pm) -**29** (Scheme 4).^{9a} Derivatisation of the carboxylate functionality in (\pm) -**28** and analogs with an appropriate P-pocket binding element promises to generate a new class of bicyclic thrombin inhibitors; this perspective is currently being further explored.

The surprisingly low $\text{p}K_a$ value (5.2) of the tertiary amino group in the tricyclic skeleton of (\pm) -**27** was further investigated in a series of related compounds, (\pm) -**30a/b** and (\pm) -**31**. The



Scheme 4 Regioselective ring opening of the tricyclic scaffold in (±)-27 and (±)-29 under basic conditions: i, 0.05 M NaOH in THF/H₂O 2 : 1. Shown are additional comparison compounds together with the pK_a values of their tertiary amine centres. Precipitation occurred during the titration of (±)-27.

endo- ((±)-30a) and *exo*- ((±)-30b) phenyl derivatives have pK_a values of 5.63 and 5.87, respectively, reflecting a minor but distinct configurational dependency. Omitting the phenyl ring in the α -position to the tertiary amine centre has a strong effect on the pK_a value: it increases to 7.04 in compound (±)-31, lacking such substituent.

The interesting pK_a values for the tertiary amino groups shown in Table 1 and Scheme 4 warrant further discussion. Our initial hypothesis to explain the high pK_a value of (±)-28 (compared to (±)-27) mainly involved the presence of a negatively charged carboxylate residue that would stabilise the protonated amine by charge attraction. However, a more detailed analysis suggests that large charge effects are not necessary to explain the measured value. Tertiary amines typically have pK_a values around 10–10.3, and a search in the MedChem02 database³⁶ shows that the introduction of a phenyl group in the α -position to the N-atom reduces the pK_a value by typically *ca.* one unit (sometimes even slightly more), which would rationalize the pK_a value of 9.3 measured for (±)-28. Indeed, an α -phenyl effect in this order of magnitude (and even slightly larger) is evident from the comparison of the pK_a values of (±)-31 vs. (±)-30a and (±)-30b.

However, it remains to rationalise the unusually low pK_a values of the tertiary amine centre in the tricyclic scaffolds such as (±)-27 and (±)-30a/b. An important pK_a -lowering contribution arises from through-bond σ -effects of the two imide carbonyl units on the amine. A search in the MedChem02 Database revealed substantial effects on amine basicities: introducing a keto function in the β -position to a saturated amine (structural element N–C(sp³)–C(sp³)–C=O) results in a lowering of the amine pK_a by *ca.* 1.5 units! Examples are the change from piperidine (pK_a 11.1) to 2-(2'-oxopropyl)piperidine (pK_a 9.45) or from 2,2,6,6-tetramethylpiperidine (pK_a 11.1) to 4-oxo-2,2,6,6-tetramethylpiperidine (pK_a 7.9). Note that in the latter case, there are two σ -paths; therefore the σ -inductive effect is operating twice and hence the pK_a shift is $2 \times 1.5 = 3 pK_a$ units.

Thus, starting from the typical pK_a value of a trialkylamine around 10, consideration of the two σ -inductive effects (ΔpK_a : 2×1.5 units) of the β -carbonyl groups leads to the pK_a value (7.04) of (±)-31. Taking further into account the α -phenyl effect (ΔpK_a *ca.* 1 unit) gives the pK_a values measured for (±)-30a (5.63) and (±)-30b (5.87). Consideration of the larger σ -inductive effects of 4-bromo- or 4-cyano-substituted (see below) α -phenyl rings rationalises the further decrease in pK_a to a value of 5.2 in (±)-27.

Although (±)-28 features two C=O groups in the β -position too, their σ -effects are reduced since they are less electrophilic (compared to the imide function) and since such effects are better transmitted across rigid rather than flexible σ -scaffolds. Also, we do not wish to exclude some contributions from the carboxylate to the higher pK_a . Clearly, this discussion shows that inductive effects of functional groups on amine centres in bi- and tricyclic scaffolds can have a dramatic effect on their pK_a values, which is worth considering in the optimisation of the pharmacokinetic properties of a lead compound.

Following full clarification of the initially surprising discrepancies obtained during pH-titrations of acidic and basic solutions, we investigated the effects of fluorine substitution on the pK_a values. Exchanging hydrogen with fluorine in the phenylamidinium needle reduces the basicity of the amidine group. Specifically, *ortho*-fluorination decreases the pK_{a2} value more than *meta*-substitution ((±)-2 vs. (±)-8, Table 1). Not surprisingly, the pK_{a2} values of difluorinated inhibitors (±)-16, (±)-17 and (±)-18 are further reduced compared to those of the monosubstituted derivatives, with the pK_{a2} value of (±)-18 (10.06) being one magnitude lower than that of non-fluorinated (±)-1 (11.14). In parallel, the lipophilicity improves as measured by log *D* at pH 7.4 from -1.16 ((±)-1) to -0.35 ((±)-18).

The same trend (reduced pK_{a1} with increasing F-substitution) was observed for the basicity of the tertiary amine centre in the tricyclic skeleton, with one notable exception (Table 1). Introduction of one F-atom *meta* to the amidinium residue in (±)-8 expectedly decreases the pK_{a1} value to 4.10 (from 4.47 in (±)-1). In sharp contrast, introduction of a second *meta*-F-substituent in (±)-16 increases the basicity again to $pK_{a1} = 4.21$. This interesting effect was fully confirmed in the corresponding series of nitrile precursors: $pK_a = 4.12$ ((±)-7), 4.16 ((±)-12), 4.36 ((±)-22), 3.58 ((±)-23) and (±)-26).

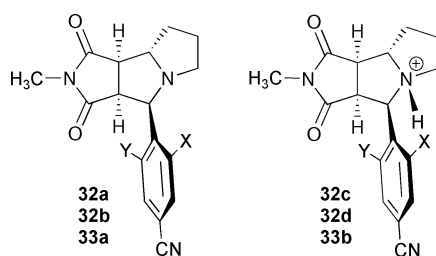
The basicity of amines is influenced by several factors: inductive and resonance effects (through bond), field effects (through space), solvation, steric hindrance and internal H-bonding.³⁷ Equilibrium geometry determinations by density functional theory (DFT) calculations (RB3LYP, 6–31G**) were conducted on the simple analogs 32a–d and 33a,b for the nitrile precursors (±)-12 and (±)-22, respectively, to shed further light onto the surprising pK_a effect. In agreement with the crystal structure analysis, it was found that conformer 32a with the *exo*-F-substituent (*exo* with respect to the dioxoperhydropyrrolo[3,4-*c*]pyrrole skeleton) is more stable than the *endo* conformer 32b by 14.2 kJ mol⁻¹ (difference in heat of formation ΔH_f° , Table 2). The *exo*-conformer observed in the crystal structure (Fig. 4) minimises 1,3-allylic-like strain and unfavorable interactions between the C–F dipole and the nitrogen lone pair.³⁹ N-Protonation reverses the stability, with the *endo*-conformer 32d now being stabilised by 17.1 kJ mol⁻¹ over the *exo*-conformer 32c as a result of favorable C–F \cdots H–N⁺ contacts.

The acid–base equilibrium of difluorinated model compound 33 was also evaluated by calculating the heats of formation of free base 33a and protonated 33b, and the data compared to the corresponding equilibrium between monofluorinated free base 32a (*exo*-F) and protonated 32d (*endo*-F; Table 2). These calculations revealed that the acid–base equilibrium of the difluorinated compound is shifted by -20.4 kJ mol⁻¹ toward

Table 2 Heats of formation ΔH_f° for unprotonated (**32a,b**, **33a**) and protonated (**32c,d**, **33b**) model compounds, obtained by DFT calculations (RB3LYP, 6-31G**)

Compound	X	Y	H_f° [Hartree] ^a
32a	H	F	-1072.0210798
32b	F	H	-1072.0156243
32c	H	F	-1072.3934282
32d	F	H	-1072.4002484
33a	F	F	-1072.2422662
33b	F	F	-1072.6293077

^a 1 Hartree = 2625 kJ mol⁻¹.



the protonated form **33b** compared with the monofluorinated system. These computational results are in agreement with the observed pK_a effects.

Finally, the crystal structure of the HCl salt of (\pm)-**22** was solved (Fig. 9). The *endo*-F(30)-atom is found in close intramolecular contacts with the H–N⁺ unit and the C-atom of the imide carbonyl group C(1)=O(6) ($d(F \cdots N^+)$ 2.83 Å, $d(F \cdots C=O)$ 3.11 Å). Similar favourable polar contacts should stabilise the *endo*-conformation of monoprotonated, monofluorinated (\pm)-**12** (and of model compound **32d**). In the crystal structure of free amine (\pm)-**22** (Fig. 5), however, the *endo*-F-atom is twisted away from the nitrogen lone pair as clearly indicated by the observed dihedral angle ω (C(23)–C(22)–C(16)–N(17)) of -54.3° , the largest in all crystal structures (see Table 3 below). F(30) is in very close intramolecular contact with the imide carbonyl group C(3)=O(7) ($d(F \cdots C=O)$ 2.74 Å) and the imide N-atom ($d(F \cdots N)$ 3.09 Å). These results indicate that the increase in basicity upon changing from (\pm)-**12** to (\pm)-**22** and from (\pm)-**8** to (\pm)-**16**, respectively, results mainly from intramolecular electrostatic field effects, *i.e.* unfavourable interactions of the C–F dipole and the nitrogen lone pair in the free base forms of (\pm)-**22** and (\pm)-**16**. In the free base forms of (\pm)-**8** and (\pm)-**12**, these interactions can be avoided by rotation of the phenyl ring.

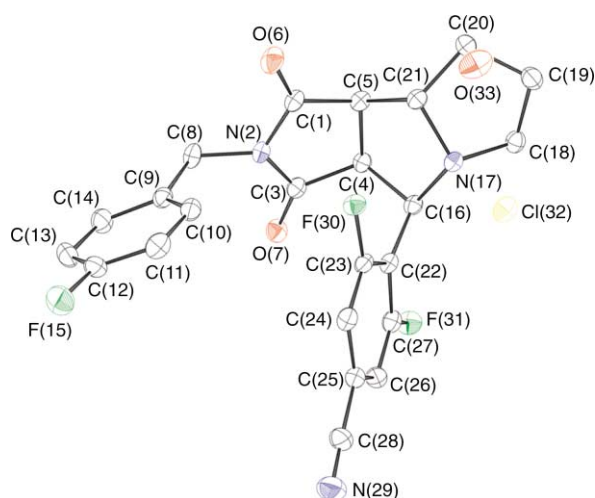
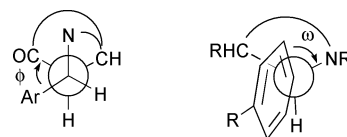


Fig. 9 ORTEP representation of the HCl salt of (\pm)-**22** with vibrational ellipsoids obtained at 223 K and shown at the 30% probability level.

Table 3 Dihedral angles describing the orientation of the phenylamidinium needle of inhibitor **1** bound in the active site of thrombin (PDB-code: 1OYT) and of benzonitrile rings as seen in crystal structures of nitrile precursors

Compound	ω	ϕ
1 ^a	29°	56°
Nitrile precursor to (\pm)- 1 ^a	40°	23°
(\pm)- 7	24°	27°
(\pm)- 12	9°	33°
(\pm)- 22	54°	31°
(\pm)- 22 ·HCl	43°	-8°

^a From ref. 9.



Influence of F-substitution on conformational properties

Exchanging H with F in the *meta* positions to the amidinium moiety in the needle influences the conformational behaviour of the inhibitor. In the ¹H NMR spectra of (\pm)-**16** and its nitrile precursor (\pm)-**22** at room temperature, the two protons *ortho* to the functional group appear as two distinct broad doublets and three fluorine signals are observed in the ¹⁹F NMR spectrum. In contrast, the two protons of (\pm)-**18** and (\pm)-**26** in the *meta* position to the amidinium/nitrile groups give one singlet and only two peaks are observed in the ¹⁹F NMR spectrum. Obviously, the barrier to rotation around the C–C bond connecting the phenyl ring to the tricyclic skeleton is increased by F-substitution in the *meta* positions, and rotation at room temperature becomes slow on the NMR time scale. By variable-temperature ¹H NMR spectroscopy, the kinetic parameters for the rotation in nitrile (\pm)-**22** were determined as $\Delta H^\ddagger = 57.0$ kJ mol⁻¹ and $\Delta S^\ddagger = -37.7$ kJ mol⁻¹.

Fig. 10 displays a succinimide ring-based overlay of the conformation of **1** bound in the active site of thrombin⁹ with the conformations of various benzonitrile precursors (nitrile precursor of (\pm)-**1**⁹ and nitriles (\pm)-**7**, (\pm)-**12**, (\pm)-**22** and (\pm)-**22**·HCl) in crystal structures. The enzyme-bound phenylamidinium needle adopts a different orientation than the benzo-

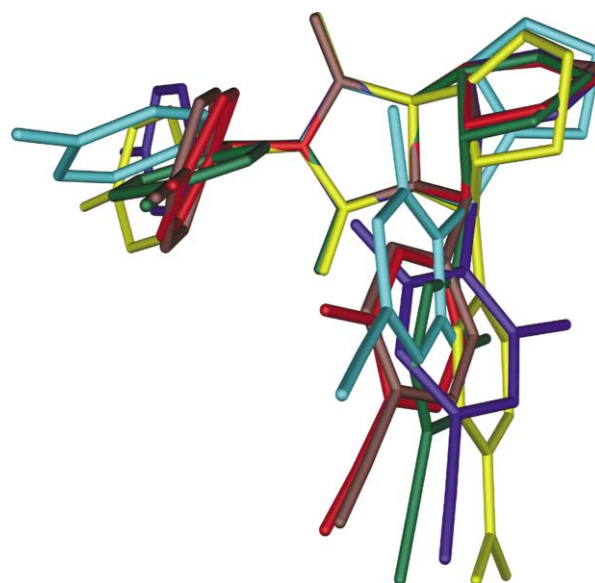


Fig. 10 Succinimide ring-based overlay of **1** (color code: yellow) bound in the active site of thrombin⁹ with the crystal structures of various benzonitrile precursors, the nitrile precursor to (\pm)-**1**⁹ (\pm)-**7** (red), (\pm)-**12** (dark green), (\pm)-**22** (blue) and (\pm)-**22**·HCl (cyan).

nitrile residues in the crystals; whether energetic costs are associated with the re-orientation, which is possibly required for binding into the S1-pocket, remains unclear. We defined two torsional angles, ω ($C_{\text{aryl}}-C_{\text{aryl}}-C(\text{sp}^3)-\text{N}$) and ϕ ($C_{\text{aryl}}-C(\text{sp}^3)-C(\text{sp}^3)-\text{CO}$) to further analyse conformational preferences of the benzonitrile rings (Table 3); however, apart from the specific geometry adopted by (\pm)-**22** to avoid repulsions between one C–F dipole and the nitrogen lone pair (see above), no particular effects resulting from F-substitution could be readily identified. It also remains unclear how the introduction of F-substituents *ortho* to the amidinium moiety affects the barrier for rotation of this group about the bond connecting it to the phenyl ring.⁴⁰

Biological results

The K_i values for the complexes of the fluorinated tricyclic inhibitors with thrombin and trypsin were determined using a chromogenic substrate (Table 1).⁴¹ The effect of F-substitution is in all cases detrimental for inhibitory activity. Introduction of one fluorine substituent in the 2- or 3-position of the phenylamidinium needle reduces the inhibitory activity by one order of magnitude. The difluorinated inhibitors are even less potent, with activities reduced up to two orders of magnitude. It is interesting to note that host–guest complexation studies with synthetic receptors came to different conclusions, namely that the strength of phenylamidinium \cdots carboxylate salt bridges is slightly increased upon *para*-substitution of the phenylamidinium moiety with electron-withdrawing groups.⁴²

The detrimental effect of fluorine substitution of the phenylamidinium needle on binding affinity is of complex origin. Several characteristics of the inhibitors, such as acid–base properties ($\text{p}K_{\text{a}1}$ and $\text{p}K_{\text{a}2}$), $\log D$ (Table 1) and conformational preferences are affected in addition to the direct interactions with the protein environment. The results are, however, in full agreement with the previously reported “ σ -effect” for substituted benzamidinium substrates,^{11–13} stating that electron-withdrawing substituents decrease biological activity. Molecular modeling using the MOLOC system⁴³ showed that the introduction of the F-substituents did not generate any repulsive van der Waals contacts, however, potentially unfavourable electrostatic contacts between 2-F (*ortho* to the amidinium) with the crystal-bound water and the carbonyl O-atom of Gly219 were identified.

Strong linear free energy relationships (LFERs) between the binding affinities ($-\Delta G$) to both enzymes and the $\text{p}K_{\text{a}}$ of the amidinium residue of the inhibitors were found (Fig. 11). At the pH (8.00) of the assay, the amidines in all inhibitors are fully protonated. Interestingly, the dependence of the binding affinity from the basicity of the amidine residues is much larger for thrombin (slope of the linear regression: 2.18) than for trypsin (slope 0.88). This means that the $\text{p}K_{\text{a}}$ of the phenylamidinium residue not only affects binding affinity but also selectivity. More basic inhibitors form more stable complexes and are more selective for thrombin over trypsin and, with decreasing $\text{p}K_{\text{a}}$, much of the selectivity is lost. The results of the LFERs presented here therefore provide a useful guideline in the design of efficient and selective thrombin inhibitors.

Conclusions

The fluorine scan of the phenylamidinium needle in a series of tricyclic thrombin inhibitors revealed that the introduction of σ -accepting F-atoms is detrimental to binding affinity, in full agreement with the previously reported “ σ -effect” of substituents in simple benzamidinium ligands.^{11–13} Improvement of the pharmacokinetic properties of thrombin inhibitors through F-substitution of the phenylamidinium needle seems therefore not to be a viable strategy despite the desirable, significant lowering of the $\text{p}K_{\text{a}}$ of the amidinium moiety. Moreover, the strong LFERs between binding affinity and $\text{p}K_{\text{a}}$ values have different

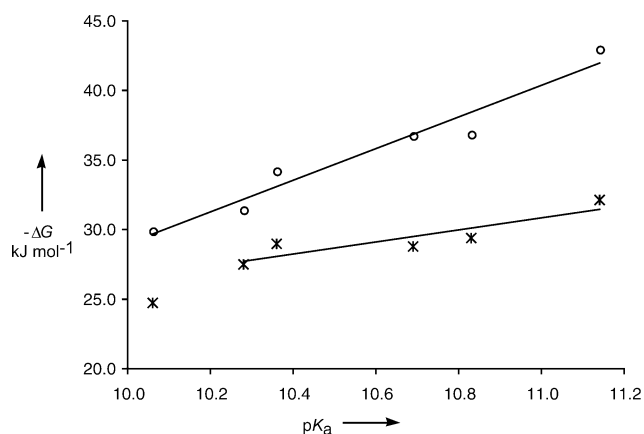


Fig. 11 Plots of the binding free enthalpies $-\Delta G$ for the complexes of the fluorinated tricyclic inhibitors with thrombin (○) and trypsin (×) against the $\text{p}K_{\text{a}2}$ values (Table 1) of the amidinium group. The data were fitted using a least-squares regression analysis. The slope of the linear free energy relationships (LFERs) is 2.18 ($R^2 = 0.97$) for thrombin and 0.88 ($R^2 = 0.86$) for trypsin. The K_i value for the complex of trypsin with (\pm)-**18** was above the threshold of the assay ($>69 \mu\text{M}$) and is therefore not included in the regression analysis.

slopes for thrombin and trypsin: decreasing the $\text{p}K_{\text{a}}$ by introduction of F-substituents affects complexation to thrombin more than to trypsin, and, as a result, binding selectivity is lost. Our data show that the “ σ -effect” of substituents on the affinity of benzamidinium needles should be rather described as a “ $\text{p}K_{\text{a}}$ -effect”.

A surprising increase in basicity of the tertiary amine centre in the tricyclic skeleton of inhibitor (\pm)-**16** (Table 1) could be explained by DFT calculations and crystal structure analysis: unfavourable interactions between a C–F dipole and the nitrogen lone pair in the free base are eliminated upon protonation.

Analysis of crystal packing environments for F-contacts revealed an extraordinarily short $C_{\text{aryl}}-\text{F} \cdots \text{H}-C_{\text{aryl}}$ interaction ($d(\text{F} \cdots \text{H}-\text{C})$ 2.22 Å), comparable to the well-described, weak $\text{O} \cdots \text{H}-\text{C}$ hydrogen bonds. Furthermore, several examples of intermolecular C–F \cdots CN contacts significantly below the sum of the van der Waals radii were observed. Additional evidence for such interactions and their orientational preferences—with the F-atom approaching the electrophilic carbon atom of the cyano group in a perpendicular fashion—was obtained by searching the CSD. This interaction bears resemblance to the multipolar C–F \cdots C=O interaction that we have previously reported.⁹

Experimental

General details

Solvents and reagents were purchased reagent-grade and used without further purification. 3-Fluoro-4-methylbenzonitrile and 4-bromo-3-fluorotoluene were purchased from ABCR, 3,5-difluorobenzaldehyde from Lancaster and 2,3-difluoro- and 3,5-difluorobenzonitrile from Acros. CH_2Cl_2 was freshly distilled from CaH_2 ; THF was distilled from Na/benzophenone. Concentration *in vacuo* is done at a pressure of ca. 20 Torr. Column chromatography (CC) on SiO_2 60 (230–400 mesh, 0.040–0.063 mm) from Fluka. TLC on SiO_2 60 F_{254} from Merck; visualisation by UV light at 245 nm. Melting points (mp) were determined with a Büchi SMP-20 apparatus and are uncorrected. In several cases, compounds decomposed (dec.) upon mp determination. IR spectra were obtained on a Perkin-Elmer 1600-FT IR instrument. ^1H , ^{13}C and ^{19}F NMR spectra were obtained on a Varian Gemini 300 or a 500 GRX Bruker spectrometer. The solvent peak was used as internal reference; for ^{19}F NMR spectra, CFCl_3 was used as internal reference. In the ^{13}C NMR spectra of (\pm)-**12** and (\pm)-**23**, one aliphatic signal

is missing and in the spectrum of (\pm)-**17**, one aromatic signal is missing, as a result of signal overlap. The exchangeable amidinium protons were not observed in ^1H NMR spectra obtained in CD_3OD . MALDI-high-resolution-mass-spectrometry (HRMS) was performed with 2,5-dihydroxybenzoic acid as matrix on a IonSpec Ultima spectrometer. Molecular ions (M^+) reported for phenylamidinium salts refer to the corresponding phenylamidinium derivatives. Elemental analyses were performed by the Mikrolabor at the Laboratorium für Organische Chemie, ETH Zürich.

4-Methyl-2-fluorobenzonitrile (**5**)¹⁷

To **4** (2.46 g, 14.0 mmol) in DMF (40 ml), CuCN (2.50 g, 28 mmol) was added. The solution was degassed and heated to reflux under Ar for 24 h. After cooling to room temperature (rt), conc. NH_3 (30 cm^3) and Et_2O (50 cm^3) were added and the mixture stirred for 1 h. After the addition of saturated (sat.) aqueous (aq.) NaCl solution (100 cm^3) and Et_2O (100 cm^3), the formed phases were separated and the aqueous phase extracted with Et_2O ($2 \times 50 \text{ cm}^3$). The combined organic phases were washed with sat. aq. NaCl solution ($2 \times 100 \text{ cm}^3$), dried (Na_2SO_4) and concentrated *in vacuo*. CC (Et_2O /pentane 1 : 5) afforded **5** (1.89 g, \approx quant.) as colourless crystals, mp 52–53 °C; δ_{H} (300 MHz; CDCl_3) 2.43 (3 H, s), 7.03 (1 H, d, J 9.6), 7.06 (1 H, d, J 9.3), 7.50 (1 H, t, J 7.5).

4-Bromomethyl-2-fluorobenzonitrile (**6**)¹⁷

To **5** (1.35 g, 10 mmol), NBS (1.87 g, 10.5 mmol) and AIBN (164 mg, 1.00 mmol) in CCl_4 (45 cm^3) were added. After heating to reflux for 8 h, the solution was filtered and the mother liquor concentrated *in vacuo*. CC (hexane/ EtOAc 6 : 1) afforded **6** (1.18 g, 55%) as colourless needles, mp 44–45 °C; δ_{H} (300 MHz; CDCl_3) 4.45 (2 H, s), 7.24–7.31 (2 H, m), 7.61 (1 H, dd, J 8.1, 6.6).

2-Fluoro-4-formylbenzonitrile (**3**)¹⁷

A solution of **6** (0.81 g, 2.8 mmol) in CH_2Cl_2 (2.3 cm^3) and Me_2SO (4.7 cm^3) was cooled to 0 °C, and TMAO·2 H_2O (1.24 g, 11.2 mmol) was added. After stirring for 5 h at 0 °C, the mixture was poured onto ice (25 cm^3) and sat. aq. NaCl solution (25 cm^3) and the aqueous phase extracted with Et_2O ($4 \times 35 \text{ cm}^3$). The combined organic phases were washed with sat. aq. NaCl solution ($2 \times 35 \text{ cm}^3$), dried (Na_2SO_4) and concentrated *in vacuo*. CC (CH_2Cl_2 /hexane 4 : 6) afforded **3** (0.31 g, 74%) as colourless needles, mp 87–88 °C; δ_{H} (300 MHz; CDCl_3) 7.73 (1 H, dd, J 8.4, 1.2), 7.80 (1 H, dd, J 7.8, 1.2), 7.85 (1 H, dd, J 7.8, 5.7), 10.06 (1 H, d, J 1.8).

2-Fluoro-4-[(3aSR,4RS,8aSR,8bRS)-2-(4-fluorobenzyl)-1,3-dioxodecahydropyrrolo[3,4-*a*]pyrrolizin-4-yl]benzonitrile ((\pm)-**7**)

Compound (\pm)-**7** was synthesised from **3** according to the procedure described below for (\pm)-**12**. CC ($2 \times$; EtOAc /hexane 55 : 45 and $\text{EtOAc}/\text{CH}_2\text{Cl}_2$ 3 : 97) followed by recrystallisation (EtOAc /hexane) afforded (\pm)-**7** (102 mg, 14%) as colourless crystals, mp 155–156 °C; ν_{max} (KBr)/ cm^{-1} 2234, 1772, 1708, 1621, 1604, 1570, 1512, 1430, 1397, 1339, 1228, 1172, 1160; δ_{H} (300 MHz; CDCl_3) 1.60–1.88 (2 H, m), 1.95–2.22 (2 H, m), 2.52–2.62 (1 H, m), 2.81–2.93 (1 H, m), 3.31 (1 H, dd, J 8.1, 0.6), 3.53 (1 H, t, J 8.3), 3.75 (1 H, dd, J 10.1, 7.4), 4.10 (1 H, d, J 8.7), 4.45, 4.51 (2 H, AB, J 14.1), 6.93–7.02 (2 H, m), 7.05–7.14 (2 H, m), 7.22–7.30 (2 H, m), 7.48 (1 H, dd, J 8.1, 6.6); δ_{C} (75 MHz; CDCl_3) 23.4, 29.7, 41.8, 48.9, 48.9, 50.4, 50.8, 67.9, 100.3 (d, J 15.8), 113.9, 115.3 (d, J 21.8), 115.8 (d, J 20.6), 124.4 (d, J 3.0), 130.5 (d, J 8.5), 131.2 (d, J 3.7), 132.8, 147.2 (d, J 7.3), 162.2 (d, J 245.4), 162.8 (d, J 256.9), 174.4, 177.2; δ_{F} (282 MHz; $\text{CDCl}_3 + \text{CFCl}_3$) –105.9 (1 F, dd, J 9.6, 6.5), –113.5 (1 F, m); HRMS calcd for $\text{C}_{23}\text{H}_{20}\text{F}_2\text{N}_3\text{O}_2^+$ ($M\text{H}^+$): 408.1524; found 408.1518; EA calcd for $\text{C}_{23}\text{H}_{19}\text{F}_2\text{N}_3\text{O}_2$ (407.41): C 67.81,

H 4.70, F 9.33, N 10.31; found: C 67.93, H 4.94, F 9.33, N 10.25%.

2-Fluoro-4-[(3aSR,4RS,8aSR,8bRS)-2-(4-fluorobenzyl)-1,3-dioxodecahydropyrrolo[3,4-*a*]pyrrolizin-4-yl]benzamide hydrochloride ((\pm)-**2**)

Compound (\pm)-**2** was synthesised according to the procedure described below for (\pm)-**8** except that the mixture was allowed to stand for 3 d at 5 °C before precipitation with Et_2O . CC ($\text{CH}_2\text{Cl}_2/\text{CH}_3\text{OH}$ 99 : 10 \rightarrow 90 : 10), followed by precipitation from $\text{EtOH}/\text{Et}_2\text{O}$ gave (\pm)-**2** (65 mg, 56%) as colourless solid, mp > 212 °C (dec.); ν_{max} (KBr)/ cm^{-1} 3376, 3109, 2962, 1776, 1709, 1674, 1627, 1613, 1487, 1471, 1402, 1348, 1237, 1180; δ_{H} (300 MHz; CD_3OD) 1.70–1.90 (2 H, m), 2.01–2.16 (2 H, m), 2.56–2.66 (1 H, m), 2.80–2.94 (1 H, m), 3.47 (1 H, dd, J 7.8, 0.6), 3.69 (1 H, dd, J 9.3, 7.2), 3.78 (1 H, t, J 8.3), 4.31 (1 H, d, J 8.7), 4.47, 4.53 (2 H, AB, J 14.2), 6.99–7.09 (2 H, m), 7.21 (1 H, dd, J 11.7, 1.2), 7.24–7.30 (2 H, m), 7.32 (1 H, dd, J 8.1, 1.2), 7.56 (1 H, t, J 7.7); δ_{C} (75 MHz; CD_3OD) 24.2, 30.5, 42.4, 50.2, 51.8, 52.0, 68.9, 69.5, 116.1 (d, J 21.9), 117.0 (d, J 9.8), 117.3 (d, J 18.8), 126.1 (d, J 3.0), 130.3, 131.2 (d, J 8.0), 133.2 (d, J 3.0), 149.2 (d, J 7.9), 160.5 (d, J 251.3), 163.5 (d, J 242.9), 164.3, 176.9, 179.7; δ_{F} (282 MHz; $\text{CD}_3\text{OD} + \text{CFCl}_3$) –112.9 (1 F, dd, J 11.1, 6.9), –114.0 (1 F, m); HRMS calcd for $\text{C}_{23}\text{H}_{23}\text{F}_2\text{N}_4\text{O}_2^+$ ($M\text{H}^+$): 425.1789; found 425.1780.

4-Bromomethyl-3-fluorobenzonitrile (**11**)²⁰

A mixture of **10** (1.15 g, 8.5 mmol), NBS (1.51 g, 8.5 mmol) and AIBN (140 mg, 0.85 mmol) in CCl_4 (40 cm^3) was heated to reflux for 8 h. Filtration and evaporation of the filtrate *in vacuo*, followed by CC (hexane/ EtOAc 9 : 1) provided **11** (1.11 g, 61%) as colourless needles, mp 75–76 °C; δ_{H} (300 MHz; CDCl_3) 4.50 (2 H, s), 7.38 (1 H, dd, J 9.3, 1.5), 7.46 (1 H, dd, J 7.8, 1.5), 7.53 (1 H, t, J = 7.8).

3-Fluoro-4-formylbenzonitrile (**9**)

A solution of **11** (0.81 g, 3.8 mmol) in CH_2Cl_2 (3 cm^3) and Me_2SO (6 cm^3) was cooled to 0 °C, and TMAO·2 H_2O (1.69 g, 15.2 mmol) was added. After stirring for 5 h at 0 °C, the mixture was poured onto ice (30 cm^3) and sat. aq. NaCl solution (30 cm^3) and the aqueous phase extracted with Et_2O ($4 \times 45 \text{ cm}^3$). The combined organic phases were washed with sat. aq. NaCl solution ($2 \times 45 \text{ cm}^3$), dried (Na_2SO_4) and concentrated *in vacuo* to give **9** (0.41 g, 73%) as colourless needles, mp 76–77 °C; δ_{H} (300 MHz; CDCl_3) 7.53 (1 H, dd, J 9.3, 1.2), 7.59 (1 H, dd, J 8.1, 0.6), 8.00 (1 H, dd, J 7.8, 7.5), 10.41 (1 H, s).

3-Fluoro-4-[(3aSR,4RS,8aSR,8bRS)-2-(4-fluorobenzyl)-1,3-dioxodecahydropyrrolo[3,4-*a*]pyrrolizin-4-yl]benzonitrile ((\pm)-**12**)

A mixture of **9** (358 mg, 2.40 mmol), *N*-(4-fluorobenzyl)-maleimide (492 mg, 2.40 mmol) and *L*-proline (276 mg, 2.40 mmol) in MeCN (7.4 cm^3) was stirred under reflux for 10 h. After cooling to rt and filtration, the filtrate was concentrated *in vacuo* and CC (EtOAc /hexane) (6 : 4) followed by recrystallisation (EtOAc /hexane) afforded (\pm)-**12** (211 mg, 22%) as colourless crystals, mp 159–160 °C; ν_{max} (KBr)/ cm^{-1} 2230, 1778, 1707, 1607, 1573, 1515, 1498, 1429, 1418, 1400, 1342, 1232, 1181, 1160; δ_{H} (300 MHz; CDCl_3) 1.63–1.88 (2 H, m), 1.96–2.22 (2 H, m), 2.56–2.66 (1 H, m), 2.86–2.98 (1 H, m), 3.33 (1 H, d, J 7.8), 3.67 (1 H, t, J 8.3), 3.76 (1 H, dd, J 10.1, 7.4), 4.30 (1 H, d, J 8.4), 4.45 (2 H, s), 6.90–6.99 (2 H, m), 7.17–7.24 (2 H, m), 7.26–7.34 (2 H, m), 7.40 (1 H, t, J 7.5); δ_{C} (75 MHz; CDCl_3) 23.5, 29.8, 41.7, 48.6, 51.0, 61.8, 67.8, 112.3 (d, J 9.7), 115.2 (d, J 21.2), 117.6 (d, J 3.0), 118.0 (d, J 24.9), 128.0 (d, J 3.7), 129.2 (d, J 4.9), 130.5 (d, J 8.5), 131.3 (d, J 3.1), 131.8 (d, J 13.4), 160.6 (d, J 24.0), 162.2 (d, J 245.0), 174.5, 177.3; δ_{F} (282

MHz; $\text{CDCl}_3 + \text{CFCl}_3$) -113.6 (1 F, m), -114.4 (1 F, s, br); HRMS calcd for $\text{C}_{23}\text{H}_{20}\text{F}_2\text{N}_3\text{O}_2^+$ (MH^+): 408.1524; found 408.1515.

3-Fluoro-4-[(3aSR,4RS,8aSR,8bRS)-2-(4-fluorobenzyl)-1,3-dioxodecahydropyrrolo[3,4-*a*]pyrrolizin-4-yl]benzamide hydrochloride (\pm)-8

To a 10 cm^3 oven-dried flask, CH_2Cl_2 (1.0 cm^3) and MeOH (1.0 cm^3) were added under N_2 and the solution cooled to 0 °C. AcCl (1.0 cm^3) was added dropwise and, after 5 min, (\pm)-11 (101 mg, 0.25 mmol) in CH_2Cl_2 (0.5 cm^3) was added and the mixture allowed to stand for 36 h at 5 °C. The formed imidate precipitated out as a white solid upon addition of Et_2O (15 cm^3) and was washed with Et_2O ($2 \times 15 \text{ cm}^3$) and dried *in vacuo*. To the imidate, MeOH (0.5 cm^3) and a 2.0 M methanolic solution of NH_3 (0.5 cm^3 , 1 mmol) were added and the mixture was stirred for 3.5 h at 65 °C. After cooling, NH_4Cl was precipitated out by addition of acetone (15 cm^3). The filtrate was concentrated *in vacuo* and the residue purified by CC ($\text{CH}_2\text{Cl}_2/\text{MeOH}$ 99 : 1 \rightarrow 90 : 10). The product was dissolved in EtOH (0.5 cm^3) and re-precipitation with Et_2O yielded (\pm)-8 (91 mg, 79%) as a colourless solid, mp >160 °C (dec.); $\nu_{\text{max}}(\text{KBr})/\text{cm}^{-1}$ 3380, 3067, 2960, 1772, 1705, 1606, 1512, 1484, 1433, 1400, 1344, 1223, 1176; $\delta_{\text{H}}(300 \text{ MHz}; \text{CD}_3\text{OD})$ 1.76–1.92 (2 H, m), 2.01–2.21 (2 H, m), 2.60–2.71 (1 H, m), 2.89–3.01 (1 H, m), 3.49 (1 H, dd, J 8.0, 0.8), 3.73 (1 H, dd, J 9.6, 7.2), 3.85 (1 H, t, J 8.1), 4.40–4.52 (3 H, m), 6.98–7.07 (2 H, m), 7.16–7.25 (2 H, m), 7.46 (1 H, dd, J 8.1, 2.0), 7.51–7.59 (2 H, m); $\delta_{\text{C}}(75 \text{ MHz}; \text{CD}_3\text{OD})$ 24.4, 30.6, 42.3, 50.0, 50.3, 52.2, 63.2, 69.3, 115.3 (d, J 24.9), 116.0 (d, J 21.8), 124.5 (d, J 3.0), 129.8 (d, J 8.5), 130.6 (d, J 4.8), 131.0 (d, J 8.5), 133.1 (d, J 3.0), 134.1 (d, J 14.0), 162.4 (d, J 245.9), 163.4 (d, J 242.8), 166.9, 176.7, 179.7; $\delta_{\text{F}}(282 \text{ MHz}; \text{CD}_3\text{OD} + \text{CFCl}_3)$ -113.7 (1 F, s, br), -114.2 (1 F, m); HRMS calcd for $\text{C}_{23}\text{H}_{23}\text{F}_2\text{N}_4\text{O}_2^+$ (MH^+): 425.1789; found 425.1787.

3,5-Difluoro-4-formylbenzonitrile (13)

To Pr_2NH (0.392 cm^3 , 2.8 mmol) in THF (5.0 cm^3) at 0 °C under Ar, 1.6 M *n*-BuLi in hexane (1.56 cm^3 , 2.5 mmol) was added dropwise over 5 min. After 10 min, the mixture was cooled to -78 °C and **19** (348 mg, 2.5 mmol) in THF (2 cm^3) added dropwise over 5 min. After stirring for 1 h at -78 °C, DMF (0.232 cm^3 , 3.0 mmol) was added dropwise over 5 min and the mixture stirred for 45 min. AcOH (0.5 cm^3) and H_2O (13 cm^3) were added and the cold solution extracted with Et_2O ($4 \times 10 \text{ cm}^3$). The combined organic phases were washed with 0.2 M HCl (10 cm^3), H_2O (10 cm^3) and sat. aq. NaCl solution (10 cm^3), followed by drying (Na_2SO_4). Concentration *in vacuo* and CC ($\text{CH}_2\text{Cl}_2/\text{hexane}$ 6 : 4) afforded **13** (0.34 g, 82%) as colourless crystals, mp 97–98 °C; $\nu_{\text{max}}(\text{KBr})/\text{cm}^{-1}$ 2248, 1694, 1686, 1627, 1568, 1429, 1417, 1324, 1209, 1196, 1181; $\delta_{\text{H}}(300 \text{ MHz}; \text{CDCl}_3)$ 7.33 (2 H, ddd, J 13.2, 3.6, 1.8), 10.35 (1 H, s); $\delta_{\text{C}}(75 \text{ MHz}; \text{CDCl}_3)$ 115.4, 116.6 (dd, J 266.1, 6.1), 117.4 (t, J 11.3), 118.8 (t, J 12.2), 162.7 (dd, J 20.1, 9.1), 182.9 (t, J 4.2); $\delta_{\text{F}}(282 \text{ MHz}; \text{CDCl}_3 + \text{CFCl}_3)$ -110.7 (2 F, dd, J 11.6, 4.2); HR-EI-MS for $\text{C}_8\text{H}_3\text{F}_2\text{NO}^+$ (M^+): 167.0183; found 166.9772, 165.9725.

3,5-Difluoro-4-[(3aSR,4RS,8aSR,8bRS)-2-(4-fluorobenzyl)-1,3-dioxodecahydropyrrolo[3,4-*a*]pyrrolizin-4-yl]benzamide hydrochloride (\pm)-22

Compound (\pm)-22 was synthesised from **13** according to the procedure described above for (\pm)-12. CC ($2 \times$; EtOAc/hexane (1 : 1) and CH_2Cl_2), followed by recrystallisation (EtOAc/hexane) afforded (\pm)-22 as a colourless solid (300 mg, 29%), mp 165–166 °C; $\nu_{\text{max}}(\text{KBr})/\text{cm}^{-1}$ 2237, 1768, 1704, 1628, 1604, 1576, 1509, 1429, 1398, 1341, 1222; $\delta_{\text{H}}(300 \text{ MHz}; \text{CDCl}_3)$ 1.60–1.88 (2 H, m), 1.98–2.23 (2 H, m), 2.58–2.70 (1 H, m), 2.82–2.88

(1 H, m), 3.32 (1 H, dd, J 8.4, 1.5), 3.58 (1 H, t, J 8.4), 3.83 (1 H, t, J 8.4), 4.48 (1 H, d, J 8.7), 4.54, 4.60 (2 H, AB, J 13.8), 6.92–7.01 (2 H, m), 7.04 (1 H, d, br, J 10.5), 7.20 (1 H, d, br, J 9.0), 7.28–7.36 (2 H, m); $\delta_{\text{C}}(75 \text{ MHz}; \text{CDCl}_3)$ 23.8, 30.1, 42.1, 49.0, 49.6, 51.9, 60.3, 68.1, 113.0 (t, J 12.4), 114.8 (dd, J 27.3, 3.6), 115.4 (d, J 21.2), 116.3 (t, J 2.9), 116.3 (dd, J 26.6, 3.3), 120.4 (t, J 13.7), 130.7 (d, J 8.5), 131.0 (d, J 3.0), 161.0 (dd, J 248.0, 9.1), 161.8 (dd, J 256.1, 6.7), 162.2 (d, J 244.4), 175.1, 177.0; $\delta_{\text{F}}(282 \text{ MHz}; \text{CDCl}_3 + \text{CFCl}_3)$ -102.3 (1 F, t, J 7.6), -110.7 (1 F, t, J 7.6), -113.6 (1 F, m); HRMS calcd for $\text{C}_{23}\text{H}_{19}\text{F}_3\text{N}_3\text{O}_2^+$ (MH^+): 426.1429; found 426.1420; EA calcd for $\text{C}_{23}\text{H}_{18}\text{F}_3\text{N}_3\text{O}_2$ (425.40): C 64.94, H 4.26, F 9.88, N 13.40; found: C 65.07, H 4.39, F 9.65, N 13.39%.

3,5-Difluoro-4-[(3aSR,4RS,8aSR,8bRS)-2-(4-fluorobenzyl)-1,3-dioxodecahydropyrrolo[3,4-*a*]pyrrolizin-4-yl]benzamide hydrochloride (\pm)-16

Compound (\pm)-16 was synthesised from (\pm)-22 according to the procedure described above for (\pm)-8. The crude product was purified by CC ($\text{CH}_2\text{Cl}_2/\text{MeOH}$ 99 : 1 \rightarrow 90 : 10), and precipitation from EtOH/ Et_2O gave (\pm)-16 (70 mg, 58%) as a colourless solid, mp >160 °C (dec.); $\nu_{\text{max}}(\text{KBr})/\text{cm}^{-1}$ 3381, 3062, 2960, 1772, 1700, 1604, 1576, 1511, 1429, 1400, 1345, 1305, 1222, 1177; $\delta_{\text{H}}(300 \text{ MHz}; \text{CD}_3\text{OD})$ 1.72–1.91 (2 H, m), 2.02–2.21 (2 H, m), 2.64–2.76 (1 H, m), 2.82–2.94 (1 H, m), 3.50 (1 H, dd, J 8.4, 1.8), 3.73–3.86 (2 H, m, 2H), 4.53, 4.58 (2 H, AB, J 14.7), 4.65 (1 H, d, J 9.0), 6.98–7.08 (2 H, m), 7.24 (1 H, d, br, J 11.1), 7.28–7.36 (2 H, m), 7.49 (1 H, d, br, J 10.2); $\delta_{\text{C}}(75 \text{ MHz}; \text{CD}_3\text{OD})$ 24.7, 31.0, 42.7, 50.5, 51.2, 53.1, 61.5, 69.4, 112.0 (d, J 26.7), 113.2 (d, J 24.3), 116.0 (d, J 21.9), 121.7 (t, J 14.3), 130.9 (t, J 11.0), 131.5 (d, J 8.5), 132.9 (d, J 3.1), 162.5 (dd, J 247.2, 9.1), 163.1 (dd, J 253.9, 6.7), 163.5 (d, J 242.9), 165.8, 177.3, 179.4; $\delta_{\text{F}}(282 \text{ MHz}; \text{CD}_3\text{OD} + \text{CFCl}_3)$ -101.4 (1 F, dd, J 10.0, 5.8), -110.4 (1 F, dd, J 9.6, 6.5), -114.3 (1 F, m); HRMS calcd for $\text{C}_{23}\text{H}_{22}\text{F}_3\text{N}_4\text{O}_2^+$ (MH^+): 443.1695; found 443.1694.

2,3-Difluoro-4-formylbenzonitrile (14)

To Pr_2NH (1.08 cm^3 , 7.7 mmol) in THF (12.0 cm^3) at 0 °C under Ar, 1.6 M *n*-BuLi in hexane (4.40 cm^3 , 7.0 mmol) was added dropwise over 5 min. After 10 min, the mixture was cooled to -78 °C and **20** (970 mg, 7.0 mmol) in THF (5 cm^3) added dropwise over 5 min. After stirring for 1 min at -78 °C, DMF (0.812 cm^3 , 10.5 mmol) was added dropwise over 5 min and the mixture stirred for 45 min. AcOH (2.0 cm^3) and H_2O (50 cm^3) were added and the cold solution extracted with Et_2O ($3 \times 30 \text{ cm}^3$). The combined organic phases were washed with 0.2 M HCl (30 cm^3), H_2O (30 cm^3) and sat. aq. NaCl solution (30 cm^3), followed by drying (Na_2SO_4). Concentration *in vacuo* and CC ($\text{Et}_2\text{O}/\text{pentane}$ 3 : 7), followed by recrystallisation ($\text{CH}_2\text{Cl}_2/\text{pentane}$) afforded **14** (0.41 g, 35%) as colourless needles, mp 52–53 °C; $\delta_{\text{H}}(300 \text{ MHz}; \text{CDCl}_3)$ 7.54 (1 H, dddd, J 8.4, 5.1, 1.8, 0.9), 7.76 (1 H, ddd, J = 8.1, 5.4, 1.5), 10.39 (1 H, s); $\delta_{\text{C}}(75 \text{ MHz}; \text{CDCl}_3)$ 108.2 (d, J 11.6), 111.8 (d, J 3.7), 123.6 (d, J 3.7), 128.1 (d, J 4.9), 128.7 (d, J 5.5), 152.0 (dd, J 263.4, 14.0), 152.2 (dd, J 262.3, 11.5), 184.1 (dd, J 6.0, 2.5); $\delta_{\text{F}}(282 \text{ MHz}; \text{CDCl}_3 + \text{CFCl}_3)$ -128.1 (1 F, ddd, J = 20.3, 5.4, 2.0), -142.9 (1 F, ddd, J = 20.3, 5.8, 2.0); HRMS calcd for $\text{C}_8\text{H}_3\text{F}_2\text{NO}^+$ (M^+): 167.0183; found 167.0170.

2,3-Difluoro-4-[(3aSR,4RS,8aSR,8bRS)-2-(4-fluorobenzyl)-1,3-dioxodecahydropyrrolo[3,4-*a*]pyrrolizin-4-yl]benzamide hydrochloride (\pm)-23

Compound (\pm)-23 was synthesised from **14** according to the procedure described above for (\pm)-12. CC (EtOAc/hexane 1 : 1), followed by recrystallisation (EtOAc/hexane) afforded (\pm)-23 (377 mg, 37%) as colourless crystals, mp 134–135 °C; $\nu_{\text{max}}(\text{KBr})/\text{cm}^{-1}$ 2239, 1776, 1710, 1631, 1604, 1512, 1472, 1432, 1399,

1345, 1300, 1223, 1175; δ_{H} (300 MHz; CDCl_3) 1.60–1.88 (2 H, m), 1.96–2.24 (2 H, m), 2.54–2.64 (1 H, m), 2.86–2.98 (1 H, m), 3.34 (1 H, d, J 8.4), 3.67 (1 H, t, J 8.1), 3.76 (1 H, dd, J 10.1, 7.4), 4.31 (1 H, d, J 8.4), 4.43, 4.49 (2 H, AB, J 14.4), 6.90–7.01 (2 H, m), 7.13–7.30 (4 H, m); δ_{C} (75 MHz; CDCl_3) 23.4, 29.8, 41.8, 48.6, 51.1, 61.8, 67.9, 101.9 (d, J 12.2), 112.9 (d, J 3.6), 115.3 (d, J 21.2), 123.4 (t, J 3.6), 127.4 (d, J 4.2), 130.5 (t, J 7.9), 131.2 (d, J 3.1), 134.5 (d, J 10.4), 148.9 (dd, J 249.0, 11.0), 150.7 (dd, J 258.8, 14.6), 162.2 (d, J 244.7), 174.3, 177.1; δ_{F} (282 MHz; $\text{CDCl}_3 + \text{CFCl}_3$) –113.5 (1 F, m), –131.7 (1 F, dd, J 21.2, 5.4), –138.6 (1 F, d br, J 18.3); HRMS calcd for $\text{C}_{23}\text{H}_{19}\text{F}_3\text{N}_3\text{O}_2^+$ ($M\text{H}^+$): 426.1429; found 426.1426.

2,3-Difluoro-4-[(3aSR,4RS,8aSR,8bRS)-2-(4-fluorobenzyl)-1,3-dioxodecahydropyrrolo[3,4-*a*]pyrrolizin-4-yl]benzamide hydrochloride (\pm)-17

Compound (\pm)-17 was synthesised from (\pm)-23 according to the procedure described above for (\pm)-8. CC ($\text{CH}_2\text{Cl}_2/\text{MeOH}$ 99 : 1 \rightarrow 90 : 10) and precipitation from EtOH/Et₂O yielded (\pm)-17 (51 mg, 43%) as a colourless solid, mp >152 °C (dec.); ν_{max} (KBr)/ cm^{-1} 3382, 2970, 1772, 1699, 1638, 1607, 1511, 1464, 1436, 1401, 1345, 1222, 1177; δ_{H} (300 MHz; CD_3OD) 1.72–1.92 (2 H, m), 2.02–2.21 (2 H, m), 2.60–2.72 (1 H, m), 2.82–3.02 (1 H, m), 3.51 (1 H, dd, J 8.0, 0.8), 3.72 (1 H, dd, J 9.3, 7.2), 3.88 (1 H, t, J 8.3), 4.41–4.53 (3 H, m), 6.98–7.07 (2 H, m), 7.17–7.25 (2 H, m), 7.30 (1 H, d, J 8.7), 7.35 (1 H, d, J 8.7); δ_{C} (75 MHz; CD_3OD) 24.4, 30.7, 42.4, 50.0, 50.2, 52.2, 63.2, 69.4, 116.1 (d, J 21.8), 118.9 (d, J 9.7), 124.8, 131.0 (d, J 8.5), 133.1 (d, J 3.1), 135.7 (d, J 10.4), 148.6 (dd, J 238.4, 15.9), 150.5 (dd, J 235.4, 12.9), 163.4, 163.5 (d, J 243.2), 176.7, 179.6; δ_{F} (282 MHz; $\text{CD}_3\text{OD} + \text{CFCl}_3$) –114.2 (1 F, m), –138.7 (1 F, s br), –139.2 (1 F, d, J 19.2); HRMS calcd for $\text{C}_{23}\text{H}_{22}\text{F}_3\text{N}_4\text{O}_2^+$ ($M\text{H}^+$): 443.1695; found 443.1691.

2,6-Difluoro-4-formylbenzamide (15)

To a mixture of **21** (2.56 g, 18 mmol), TsOH·H₂O (17 mg, 0.09 mmol) and ethyleneglycol (2.5 cm³, 45 mmol), benzene (30 cm³) was added. After heating to reflux for 16 h using a Dean-Stark trap, the mixture was partitioned between EtOAc (30 cm³) and sat. aq. NaHCO₃ solution (30 cm³). The organic phase was washed with H₂O, dried (Mg₂SO₄) and concentrated *in vacuo* to give acetal **24** as a colourless oil that was used without further purification. To ⁱPr₂NH (2.78 cm³, 19.8 mmol) in THF (36 cm³) at 0 °C under Ar, 1.6 M *n*-BuLi in hexane (11.3 cm³, 18.0 mmol) was added dropwise over 5 min. After 10 min, the mixture was cooled to –78 °C and **24** in THF (12 cm³) added dropwise over 5 min. After stirring for 2 h at –78 °C, TsCN (3.91 g, 21.6 mmol) in THF (15 cm³) was added dropwise over 10 min and the mixture stirred for 1 h at –78 °C. The mixture was allowed to warm to rt and then partitioned between Et₂O (60 cm³) and H₂O (60 cm³). The aqueous phase was extracted with Et₂O (3 × 40 cm³), and the combined organic phases were washed with 1 M HCl (80 cm³), H₂O (80 cm³) and sat. aq. NaCl solution (80 cm³). Concentration *in vacuo* afforded crude **25**, to which THF (60 cm³) and 2 M HCl (30 cm³) were added. The solution was heated to reflux for 6 h and, after cooling to rt, Et₂O (60 cm³) was added and the two phases were separated. The aqueous phase was extracted with Et₂O (2 × 60 cm³), and the combined organic phases were washed with sat. aq. NaHCO₃ solution (80 cm³), H₂O (80 cm³) and sat. aq. NaCl solution (80 cm³). Drying (Na₂SO₄), concentration *in vacuo* and CC (Et₂O/pentane 3 : 7) afforded **15** (1.43 g, 48%) as colourless needles, mp 48–50 °C; δ_{H} (300 MHz; CDCl_3) 7.58 (2 H, ddd, J 9.0, 1.5, 0.9), 10.00 (1 H, t, J 1.8); δ_{C} (75 MHz; CDCl_3) 97.5 (t, J 16.7), 108.2, 112.4 (dd, J 20.7, 3.6), 141.4 (t, J 7.3), 163.5 (dd, J 264.1, 3.6), 187.5; δ_{F} (282 MHz; $\text{CDCl}_3 + \text{CFCl}_3$) –100.0 (2 F, t, J 7.3); HRMS calcd for $\text{C}_8\text{H}_5\text{F}_2\text{NO}^+$ (M^+): 167.0183; found 167.0142.

2,6-Difluoro-4-[(3aSR,4RS,8aSR,8bRS)-2-(4-fluorobenzyl)-1,3-dioxodecahydropyrrolo[3,4-*a*]pyrrolizin-4-yl]benzamide (\pm)-26

Compound (\pm)-26 was synthesised according to the procedure described above for (\pm)-12. CC (2 ×; EtOAc/hexane 40 : 60 and EtOAc/ CH_2Cl_2 10 : 90) followed by recrystallisation (EtOAc/hexane) provided (\pm)-26 (154 mg, 15%) as colourless crystals, mp 169–170 °C; ν_{max} (KBr)/ cm^{-1} 2238, 1773, 1706, 1632, 1628, 1605, 1576, 1572, 1511, 1441, 1400, 1344, 1230, 1172; δ_{H} (300 MHz; CDCl_3) 1.58–1.71 (1 H, m), 1.72–1.88 (1 H, m), 1.95–2.23 (2 H, m), 2.50–2.61 (1 H, m), 2.82–2.94 (1 H, m), 3.32 (1 H, d, J 8.1), 3.53 (1 H, t, J 8.4), 3.74 (1 H, dd, J 9.4, 7.5), 4.07 (1 H, d, J 8.4), 4.47, 4.52 (2 H, AB, J 14.1), 6.92 (2 H, d, J 8.7), 6.94–7.03 (2 H, m), 7.28–7.36 (2 H, m); δ_{C} (75 MHz; CDCl_3) 23.5, 29.8, 41.9, 48.8, 50.4, 50.9, 68.0, 68.1, 91.4 (t, J 19.4), 109.3, 111.5 (dd, J 20.6, 3.4), 115.5 (d, J 21.2), 130.5 (t, J 8.6), 131.1 (d, J 3.6), 148.7 (t, J 8.8), 162.3 (d, J 245.0), 162.7 (dd, J 259.0, 4.9), 174.2, 176.9; δ_{F} (282 MHz; $\text{CDCl}_3 + \text{CFCl}_3$) –110.4 (2 F, d, J 8.5), –113.3 (1 F, m); HRMS calcd for $\text{C}_{23}\text{H}_{19}\text{F}_3\text{N}_3\text{O}_2^+$ ($M\text{H}^+$): 426.1429; found 426.1420.

2,6-Difluoro-4-[(3aSR,4RS,8aSR,8bRS)-2-(4-fluorobenzyl)-1,3-dioxodecahydropyrrolo[3,4-*a*]pyrrolizin-4-yl]benzamide hydrochloride (\pm)-18

A solution of (\pm)-26 (106 mg, 0.25 mmol), NH₂OH·HCl (48 mg, 0.5 mmol) and Et₃N (104 cm³, 0.75 mmol) in MeOH (0.5 cm³) and THF (2 cm³) was stirred for 16 h after which it was partitioned between CH_2Cl_2 (15 cm³) and H₂O (15 cm³). The organic phase was washed with H₂O (15 cm³), dried (Na₂SO₄) and concentrated *in vacuo*. The residual solid was taken up in AcOH (2 cm³), and Ac₂O (35 cm³, 0.38 mmol) was added. After stirring for 5 min, Pd/C (10%, 15 mg) was added and hydrogenation (H₂ balloon) conducted for 5 h. Filtration through Celite, concentration and CC ($\text{CH}_2\text{Cl}_2/\text{MeOH}$ 99 : 1 \rightarrow 90 : 10), followed by precipitation from HCl/EtOH/Et₂O afforded (\pm)-18 (47 mg, 39%) as colourless solid, mp >171 °C (dec.); ν_{max} (KBr)/ cm^{-1} 3389, 3048, 2973, 1773, 1705, 1692, 1641, 1604, 1512, 1467, 1435, 1402, 1346, 1224, 1177; δ_{H} (500 MHz; $\text{CD}_3\text{OD} + \text{TMS}$) 1.72–1.88 (2 H, m), 2.02–2.14 (2 H), 2.54–2.63 (1 H, m), 2.83–2.93 (1 H, m), 3.46 (1 H, d, J 8.0), 3.69 (1 H, dd, J 9.6, 7.4), 3.74 (1 H, t, J 8.3), 4.27 (1 H, d, J 8.7), 4.47, 4.55 (2 H, d, J 14.5), 7.00–7.07 (2 H, m), 7.10 (2 H, d br, J 9.8), 7.23–7.32 (2 H, m); δ_{C} (125 MHz; $\text{CD}_3\text{OD} + \text{TMS}$) 24.2, 30.5, 42.5, 50.1, 51.8, 51.9, 68.9, 69.6, 107.7 (t, J 19.3), 113.1 (dd, J 22.1, 2.9), 116.3 (d, J 21.8), 131.3 (d, J 7.5), 133.4 (d, J 3.2), 149.9 (t, J 9.2), 160.1, 160.4 (dd, J 253.4, 5.9), 163.8 (d, J 245.0), 177.2, 179.8; δ_{F} (282 MHz; $\text{CD}_3\text{OD} + \text{CFCl}_3$) –111.7 (2 F, d, J 9.6), –114.1 (1 F, m); HRMS calcd for $\text{C}_{23}\text{H}_{22}\text{ClF}_3\text{N}_4\text{O}_2^+$ ($M\text{H}^+$): 443.1695; found 443.1694.

(3aSR,4RS,8aSR,8bRS)-2-(4-Fluorobenzyl)-4-phenylhexahydropyrrolo[3,4-*a*]pyrrolizine-1,3(2H,4H)-dione (\pm)-30a and (3aSR,4SR,8aRS,8bRS)-2-(4-Fluorobenzyl)-4-phenylhexahydropyrrolo[3,4-*a*]pyrrolizine-1,3(2H,4H)-dione (\pm)-30b

Compounds (\pm)-30a and (\pm)-30b were synthesised according to the procedure described above for (\pm)-12 from *N*-(4-fluorobenzyl)maleimide (307 mg, 1.5 mmol), L-proline (173 mg, 1.5 mmol) and benzaldehyde (159 mg, 1.5 mmol). CC ($\text{CH}_2\text{Cl}_2/\text{EtOAc}$ 100 : 0 \rightarrow 70 : 30) afforded (\pm)-30a (220 mg, 40%) as colourless needles, mp 109–110 °C and (\pm)-30b (200 mg, 37%) as a yellow oil. (\pm)-30a: ν_{max} (neat)/ cm^{-1} 1772, 1698, 1603, 1510, 1430, 1397, 1340, 1221, 1169. δ_{H} (300 MHz; CDCl_3) 1.60–1.85 (2 H, m), 1.96–2.19 (2 H, m), 2.62–2.77 (1 H, m), 2.80–2.94 (1 H, m), 3.32 (1 H, dd, J 7.8, 0.6), 3.49 (1 H, t, J 8.4), 3.74 (1 H, dd, J 9.6, 6.9), 4.08 (1 H, d, J 8.7), 4.50 (2 H, s), 6.94–7.03 (2 H, m), 7.18–7.33 (7 H, m); δ_{C} (75 MHz; CDCl_3) 23.4, 29.6, 41.7, 49.0, 50.6, 50.7, 67.8, 68.7, 115.2 (d, J 21.4), 127.7, 127.8, 128.0, 130.7 (t, J 8.5), 131.5 (d, J 3.0), 137.6, 162.2 (d, J 246.0), 175.0,

177.8; δ_{F} (282 MHz; $\text{CDCl}_3 + \text{CFCl}_3$) -114.1 (1 F, m); HRMS calcd for $\text{C}_{22}\text{H}_{22}\text{FN}_2\text{O}_2^+$ ($M\text{H}^+$): 365.1660; found 365.1655. (\pm)-**30b**: $\nu_{\text{max}}(\text{neat})/\text{cm}^{-1}$ 1771, 1697, 1603, 1509, 1431, 1393, 1339, 1222, 1158; δ_{H} (300 MHz; CDCl_3) 1.55–1.78 (3 H, m), 1.88–2.00 (1 H, m), 2.38–2.47 (1 H, m), 2.88–2.98 (1 H, m), 3.35 (1 H, dd, J 9.0, 5.1), 3.51 (1 H, t, J 9.0), 3.84–3.94 (1 H, m), 4.13 (1 H, d, J 5.1), 4.61 (2 H, s), 6.95–7.04 (2 H, m), 7.22–7.48 (7 H, m); δ_{C} (75 MHz; CDCl_3) 24.2, 26.2, 41.8, 48.0, 52.1, 55.6, 66.3, 69.5, 115.4 (d, J 21.4), 126.6, 127.3, 128.5, 130.8 (t, J 8.5), 131.2 (d, J 3.0), 141.9, 162.2 (d, J 246.0), 176.5, 177.6; δ_{F} (282 MHz; $\text{CDCl}_3 + \text{CFCl}_3$) -113.3 (1 F, m); HRMS calcd for $\text{C}_{22}\text{H}_{22}\text{FN}_2\text{O}_2^+$ ($M\text{H}^+$): 365.1660; found 365.1656.

(3aSR,8aSR,8bRS)-2-(4-Fluorobenzyl)hexahydropyrrolo-[3,4-*a*]pyrrolizin-1,3(2H,4H)-dione (\pm)-**31**

Compound (\pm)-**31** was synthesised according to the procedure described above for (\pm)-**12** from *N*-(4-fluorobenzyl)maleimide (307 mg, 1.5 mmol), *L*-proline (173 mg, 1.5 mmol) and paraformaldehyde (45 mg, 1.5 mmol). CC ($\text{EtOAc}/\text{Et}_3\text{N}$ 97.5 : 2.5) afforded (\pm)-**31** (116 mg, 27%) as a slightly yellow oil; $\nu_{\text{max}}(\text{neat})/\text{cm}^{-1}$ 1772, 1696, 1603, 1510, 1430, 1397, 1340, 1220, 1166; δ_{H} (300 MHz; CDCl_3) 1.50–1.80 (2 H, m), 1.90–2.10 (2 H, m), 2.70–2.92 (3 H, m), 3.11 (1 H, dd, J 8.1, 2.1), 3.23 (1 H, dd, J 10.2, 2.1), 3.31 (1 H, td, J 8.1, 2.1), 4.08 (1 H, m), 4.57 (2 H, s), 6.89–6.98 (2 H, m), 7.25–7.34 (2 H, m); δ_{C} (75 MHz; CDCl_3) 23.6, 29.6, 41.7, 45.9, 50.0, 51.8, 54.5, 68.7, 115.2 (d, J 21.4), 130.2 (d, J 7.5), 131.4 (d, J 3.0), 137.6, 162.0 (d, J 246.0), 177.7, 178.2; δ_{F} (282 MHz; $\text{CDCl}_3 + \text{CFCl}_3$) -114.0 (1 F, m); HRMS calcd for $\text{C}_{16}\text{H}_{18}\text{FN}_2\text{O}_2^+$ ($M\text{H}^+$): 289.1347; found 289.1350.

Imide opening under basic conditions

Solutions of (\pm)-**27**^{7d} in THF (1.22 cm³) and NaOH (16 mg, 0.4 mmol) in H₂O (0.66 cm³) were stirred together at rt. After 1 h, only traces of starting material were detected by TLC. After 2 h, the solution was concentrated *in vacuo* and re-concentrated after addition of toluene (3 \times) to give (\pm)-**28** in a quantitative conversion (¹H NMR); $\nu_{\text{max}}(\text{neat})/\text{cm}^{-1}$ 1622, 1578 (s), 1603, 1446, 1416, 1356, 1227, 1110; δ_{H} (300 MHz; CD_3OD) 1.80–2.12 (2 H, m), 2.20–2.34 (1 H, m), 2.50–2.60 (1 H, m), 2.94–3.05 (2 H, m), 3.13 (1 H, dd, J 9.0, 6.9), 3.74 (1 H, t, J 5.7), 4.33 (1 H, d, J 5.7), 4.38–4.48 (1 H, m), 4.07, 4.53 (2 H, AB, J 13.3), 6.89–6.98 (5 H, m), 7.25–7.34 (4 H, m); δ_{C} (75 MHz; D_2O) 33.3, 33.4, 42.8, 54.3, 56.7, 57.6, 57.7, 72.8, 120.3, 126.4, 127.7, 128.2, 130.2, 131.2, 139.3, 140.7, 172.4, 178.7; HRMS calcd for $\text{C}_{22}\text{H}_{24}\text{BrN}_2\text{O}_3^+$ ($M\text{H}^+$): 443.0970, 445.0950; found 443.0960, 445.0944. The imide ring opening of (\pm)-**29** (5 mg, 0.012 mmol) in D₂O (0.9 cm³) and 0.5 M NaOD (0.1 cm³) was also monitored and confirmed by ¹H NMR.

Computational investigation

The enthalpy of formation ΔH_{f} of the different conformers of **32** and **33** in unprotonated and protonated forms was obtained by calculating the equilibrium geometry in Spartan⁰⁴³⁸ utilising density functional theory and a 6-31G** basis set.

High-throughput log *D* screening

The applied high-throughput (HT) method for the determination of the distribution coefficient HT-log *D* is based on microplate technique and derived from the conventional ‘shake flask’ method. The compound is distributed between H₂O buffered at a specific pH and 1-octanol. The distribution coefficient is then calculated from the difference in concentration in the aqueous phase before and after partitioning and the ratio of the two phases. The ‘one phase-analysed’ experiment starts with a pure Me₂SO solution of the lead molecule of interest which is dispensed in aqueous buffer with *c* (compound) = 0.5 mM. A part of this solution is then analysed by measuring the

UV absorption. The obtained optical density (reference) is equal to the concentration of the substance before partitioning. An exact amount of 1-octanol is added and the mixture incubated by quiet shaking (2 h). The emulsion is allowed to stand overnight to be sure that the partition equilibrium is reached. The next day, the layers need thorough centrifugation at 3000 rpm for 10 min and the concentration of the substance in the aqueous phase is determined again by measuring the UV absorption. The procedure above is carried out at four different octanol/water ratios, two with a large volume of octanol for hydrophilic compounds (log *D* < 1) and two with a low volume of octanol for the lipophilic compounds (log *D* > 1).

p*K*_a Determination by potentiometric titration⁴⁴

The p*K*_a values (reproducibility: ± 0.05 units) were determined by potentiometric titrations using GLp*K*_a from Sirius Analytical Instruments Ltd. In the applied pH-metric method, a solution of the sample is titrated over a pH range in which it passes from being fully protonated to fully deprotonated. The p*K*_a values are calculated by analysing the shape of the titration curve. General titration procedure: An exact amount of the sample is placed directly into the vial. The instrument adds 0.1 M KNO₃ (20 cm³) as background electrolyte. It then checks the pH of the sample solution and adds 0.5 M HCl to bring the pH down to the initial pH 2. It then titrates with standardised base solution (0.5 M KOH) until the final pH value of 12 has been reached, at which point data collection is terminated. The titration is running under argon atmosphere to minimise absorption of atmospheric CO₂ because of the p*K*_a values of carbonate. This procedure results in a data set containing a single potentiometric titration curve. The data set is downloaded to the computer, and p*K*_a results are calculated by p*K*_a-LOGP V5.2a. In comparison with a blank titration (without sample), the shape of such a curve indicates the amount of substance present and its characteristic acid–base ionisation properties.

Crystal structures

The crystal structures were solved by direct methods⁴⁵ and refined by full-matrix least-squares analysis⁴⁶ (heavy atoms anisotropic, H-atoms isotropic, whereby H-positions are based on stereochemical considerations). †

Crystal data of (\pm)-**7** at 223 K: $\text{C}_{23}\text{H}_{19}\text{F}_2\text{N}_3\text{O}_2$, (M_{r} = 407.41); triclinic, space group $P\bar{1}$, D_{c} = 1.404 g cm⁻³, Z = 2, a = 9.4926(2), b = 10.3004(3), c = 10.9831(3) Å, α = 93.680(1)°, β = 94.130(1)°, γ = 115.220(1)°, V = 963.64(4) Å³. Linear crystal dimensions *ca.* 0.3 \times 0.3 \times 0.25 mm. Bruker-Nonius Kappa-CCD, Mo*K*_α radiation, λ = 0.7107 Å. Final $R(F)$ = 0.0437, $wR(F^2)$ = 0.1161 for 291 parameters and 3458 reflections with $I > 2\sigma(I)$ and $\theta < 27.49^\circ$. CCDC 231344.

Crystal data of (\pm)-**12** at 223 K: $\text{C}_{23}\text{H}_{19}\text{F}_2\text{N}_3\text{O}_2$, (M_{r} = 407.41); triclinic, space group $P\bar{1}$, D_{c} = 1.373 g cm⁻³, Z = 2, a = 7.673(1), b = 11.394(2), c = 11.894(2) Å, α = 97.22(1)°, β = 106.92(1)°, γ = 90.85(1)°, V = 985.5(3) Å³. Linear crystal dimensions *ca.* 0.22 \times 0.2 \times 0.18 mm. Nonius CAD4 diffractometer, Cu*K*_α radiation, λ = 1.5418 Å. Final $R(F)$ = 0.0449, $wR(F^2)$ = 0.1256 for 291 parameters and 3272 reflections with $I > 2\sigma(I)$ and $\theta < 74.9^\circ$. CCDC 231343.

Crystal data of **13** at 100 K: $\text{C}_8\text{H}_3\text{F}_2\text{NO}$, (M_{r} = 167.11); orthorhombic, space group $P2_12_12_1$, D_{c} = 1.660 g cm⁻³, Z = 4, a = 3.7369(2), b = 6.2036(3), c = 28.8526(2) Å, V = 668.87(6) Å³. Linear crystal dimensions *ca.* 0.1 \times 0.1 \times 0.07 mm. Bruker-Nonius Kappa-CCD, Mo*K*_α radiation, λ = 0.7107 Å. Final $R(F)$ = 0.0327, $wR(F^2)$ = 0.0677 for 113 parameters and 1267 reflections with $I > 2\sigma(I)$ and $\theta < 27.45^\circ$. CCDC 231345.

† CCDC reference numbers 231343–231347. See <http://www.rsc.org/suppdata/ob/b4/b402515f/> for crystallographic data in.cif or other electronic format.

Crystal data of (\pm)-**22** at 243 K: $C_{23}H_{18}F_3N_3O_2$, ($M_r = 425.40$); monoclinic, space group $P2_1/n$, $D_c = 1.452 \text{ g cm}^{-3}$, $Z = 4$, $a = 4.8890(7)$, $b = 20.180(2)$, $c = 19.844(2) \text{ \AA}$, $\beta = 96.211(5)^\circ$, $V = 1946.3(4) \text{ \AA}^3$. Linear crystal dimensions *ca.* $0.09 \times 0.07 \times 0.05 \text{ mm}$. Bruker-Nonius Kappa-CCD, MoK_α radiation, $\lambda = 0.7107 \text{ \AA}$. Final $R(F) = 0.1252$, $wR(F^2) = 0.3214$ for 299 parameters and 2225 reflections with $I > 2\sigma(I)$ and $\theta < 24.12$. CCDC 231347.

Crystal data of (\pm)-**22**·HCl at 223 K: $C_{23}H_{19}ClF_3N_3O_2 + H_2O$ ($M_r = 479.88$); monoclinic, space group $P2_1/c$, $D_c = 1.496 \text{ g cm}^{-3}$, $Z = 4$, $a = 11.6360(6)$, $b = 6.9444(4)$, $c = 26.6949(16) \text{ \AA}$, $\beta = 98.983(2)^\circ$, $V = 2130.63(17) \text{ \AA}^3$. Linear crystal dimensions *ca.* $0.1 \times 0.1 \times 0.03 \text{ mm}$. Bruker-Nonius Kappa-CCD, MoK_α radiation, $\lambda = 0.7107 \text{ \AA}$. Final $R(F) = 0.0664$, $wR(F^2) = 0.1639$ for 321 parameters and 2354 reflections with $I > 2\sigma(I)$ and $\theta < 24.11^\circ$. CCDC 231346.

Acknowledgements

We thank Dr. F. Hof (ETH Zürich) for assistance with the DFT calculations and manuscript corrections, Prof. B. Jaun (ETH Zürich) for advice with the NMR experiments and Dr. C. Thilgen (ETH Zürich) for help with the nomenclature. The research was supported by the ETH research council, F. Hoffmann-La Roche Ltd and the Carlsberg Foundation (postdoctoral fellowship to J.A.O.).

References

- 1 J. Fried and E. F. Sabo, *J. Am. Chem. Soc.*, 1954, **76**, 1455–1456.
- 2 F. M. D. Ismael, *J. Fluorine Chem.*, 2002, **118**, 27–33.
- 3 M. Schlosser, in *Enantiocontrolled Synthesis of Fluoro-Organic Compounds: Stereochemical Challenges and Biomedical Targets*, ed. V. A. Soloshonok, Wiley, Chichester, 1999, pp 613–659.
- 4 C. M. Weeks, W. L. Duax and M. E. Wolff, *J. Am. Chem. Soc.*, 1973, **95**, 2865–2868.
- 5 P. M. Matias, M. A. Carrondo, R. Coelho, M. Thomaz, X.-Y. Zhao, A. Wegg, K. Crusius, U. Egner and P. Donner, *J. Med. Chem.*, 2002, **45**, 1439–1446.
- 6 (a) B. K. Park, N. R. Kitteringham and P. M. O'Neill, *Annu. Rev. Pharmacol. Toxicol.*, 2001, **41**, 443–470; (b) D. O'Hagan and H. S. Rzepa, *Chem. Commun.*, 1997, 645–652; (c) B. E. Smart, *J. Fluorine Chem.*, 2001, **109**, 3–11.
- 7 (a) U. Obst, V. Gramlich, F. Diederich, L. Weber and D. W. Banner, *Angew. Chem., Int. Ed.*, 1995, **34**, 1739–1742; (b) U. Obst, D. W. Banner, L. Weber and F. Diederich, *Chem. Biol.*, 1997, **4**, 287–295; (c) U. Obst, P. Betschmann, C. Lerner, P. Seiler, F. Diederich, V. Gramlich, L. Weber, D. W. Banner and P. Schönholzer, *Helv. Chim. Acta*, 2000, **83**, 855–909; (d) P. Betschmann, S. Sahli, F. Diederich, U. Obst and V. Gramlich, *Helv. Chim. Acta*, 2002, **85**, 1210–1245.
- 8 B. Kuhn and P. A. Kollman, *J. Am. Chem. Soc.*, 2000, **122**, 3909–3916.
- 9 (a) J. A. Olsen, D. W. Banner, P. Seiler, U. Obst Sander, A. D'Arcy, M. Stihle, K. Müller and F. Diederich, *Angew. Chem., Int. Ed.*, 2003, **42**, 2507–2511; (b) J. A. Olsen, D. W. Banner, P. Seiler, U. Obst-Sander, A. D'Arcy, M. Stihle, K. Müller and F. Diederich, *ChemBioChem*, in press.
- 10 (a) For examples of phenylamidine-containing thrombin inhibitors, see: J. W. Nilsson, I. Kvarnstrom, D. Musil, I. Nilsson and B. Samulsson, *J. Med. Chem.*, 2003, **46**, 3985–4001; (b) S. Hanessian, E. Therrien, K. Granberg and I. Nilsson, *Bioorg. Med. Chem. Lett.*, 2002, **12**, 2907–2911; (c) N. H. Haeuël, H. Nar, H. Priepke, U. Ries, J.-M. Stassen and W. Wienen, *J. Med. Chem.*, 2002, **45**, 1757–1766; (d) for a review, see: J. B. M. Rewinkel and A. E. P. Adang, *Curr. Pharm. Des.*, 1999, **5**, 1043–1075.
- 11 R. Talhout and J. B. F. N. Engberts, *Eur. J. Biochem.*, 2001, **268**, 1554–1560.
- 12 (a) M. Recanatini, T. Klein, C.-Z. Yang, J. McClarin, R. Langridge and C. Hansch, *Mol. Pharmacol.*, 1986, **29**, 436–446; (b) D. Labes and V. Hagen, *Pharmazie*, 1979, **34**, 649–653; (c) M. Mares-Guia, D. L. Nelson and E. Rogana, *J. Am. Chem. Soc.*, 1977, **99**, 2331–2336; (d) B. A. Katz, R. Mackman, C. Luong, K. Radika, A. Martelli, P. A. Sprengeler, J. Wang, H. Chan and L. Wong, *Chem. Biol.*, 2000, **7**, 299–312.
- 13 (a) P. E. J. Sanderson, M. G. Stanton, B. D. Dorsey, T. A. Lyle, C. McDonough, W. M. Sanders, K. L. Savage, A. M. Naylor-Olsen, J. A. Krueger, S. D. Lewis, B. J. Lucas, J. J. Lynch and Y. Yan, *Bioorg. Med. Chem. Lett.*, 2003, **13**, 795–798; (b) T. J. Tucker, S. F. Brady, W. C. Lumma, S. D. Lewis, S. J. Gardell, A. M. Naylor-Olsen, Y. Yan, J. T. Sisko, K. J. Stauffer, B. J. Lucas, J. J. Lynch, J. J. Cook, M. T. Stranieri, M. A. Holahan, E. A. Lyle, E. P. Baskin, I.-W. Chen, K. B. Dancheck, J. A. Krueger, C. M. Cooper and J. P. Vacca, *J. Med. Chem.*, 1998, **41**, 3210–3219; (c) Y. St-Denis, S. Lévesque, B. Bachand, J. J. Edmunds, L. Leblond, P. Prévile, M. Tarazi, P. D. Winocour and M. A. Siddiqui, *Bioorg. Med. Chem. Lett.*, 2002, **12**, 1181–1184.
- 14 (a) B. A. Katz, P. A. Sprengeler, C. Luong, E. Verner, K. Elrod, M. Kirtley, J. Janc, J. R. Spencer, J. G. Breitenbucher, H. Hui, D. McGee, D. Allen, A. Martelli and R. L. Mackman, *Chem. Biol.*, 2001, **8**, 1107–1121; (b) K. Lee, C. W. Park, W.-H. Jung, H. D. Park, S. H. Lee, K. H. Chung, S. K. Park, O. H. Kwon, M. Kang, D.-H. Park, S. K. Lee, E. E. Kim, S. K. Yoon and A. Kim, *J. Med. Chem.*, 2003, **46**, 3612–3622.
- 15 J. W. Essex, D. L. Severance, J. Tirado-Rives and W. L. Jorgensen, *J. Phys. Chem. B*, 1997, **101**, 9663–9669.
- 16 (a) C. R. W. Guimaraes and R. B. de Alencastro, *J. Phys. Chem. B*, 2002, **106**, 466–476; (b) S. M. Schwarzl, T. M. Tschopp, J. C. Smith and S. Fischer, *J. Comput. Chem.*, 2002, **23**, 1143–1149; (c) C. F. Wong and J. A. McCammon, *J. Am. Chem. Soc.*, 1986, **108**, 3830–3832; (d) G. Náray-Szabó, *J. Am. Chem. Soc.*, 1984, **106**, 4584–4589; (e) H.-J. Henkel, D. Labes and V. Hagen, *Pharmazie*, 1983, **38**, 342–346.
- 17 C. J. Dinsmore, M. J. Bogusky, J. C. Culberson, J. M. Bergman, C. F. Homnick, C. B. Zartman, S. D. Mosser, M. D. Schaber, R. G. Robinson, K. S. Koblan, H. E. Huber, S. L. Graham, G. D. Hartman, J. R. Huff and T. M. Williams, *J. Am. Chem. Soc.*, 2001, **123**, 2107–2108.
- 18 I. M. Bell, S. N. Gallicchio, M. Abrams, L. S. Beese, D. C. Beshore, H. Bhimnathwala, M. J. Bogusky, C. A. Buser, J. C. Culberson, J. Davide, M. Ellis-Hutchings, C. Fernandes, J. B. Gibbs, S. L. Graham, K. A. Hamilton, G. D. Hartman, D. C. Heimbrook, C. F. Homnick, H. E. Huber, J. R. Huff, K. Kassahun, K. S. Koblan, N. E. Kohl, R. B. Lobell, J. J. Lynch Jr., R. Robinson, A. D. Rodrigues, J. S. Taylor, E. S. Walsh, T. M. Williams and C. B. Zartman, *J. Med. Chem.*, 2002, **45**, 2388–2409.
- 19 (a) R. Grigg, J. Idle, P. McMeekin and D. Vipond, *J. Chem. Soc., Chem. Commun.*, 1987, 49–51; (b) O. Tsuge and S. Kanemasa, *Adv. Heterocycl. Chem.*, 1989, **45**, 231–349.
- 20 C.-B. Xue, J. Wityak, T. M. Sielecki, D. J. Pinto, D. G. Batt, G. A. Cain, M. Sworin, A. L. Rockwell, J. F. Roderick, S. Wang, M. J. Orwat, W. E. Fietze, L. L. Bostrom, J. Liu, C. A. Higley, F. W. Rankin, A. E. Tobin, G. Emmett, G. K. Lalka, J. Y. Sze, S. V. Di Meo, S. A. Mousa, M. J. Thoolen, A. L. Racanelli, E. A. Hausner, T. M. Reilly, W. F. DeGrado, R. R. Wexler and R. E. Olson, *J. Med. Chem.*, 1997, **40**, 2064–2084.
- 21 A. J. Bridges, A. Lee, E. C. Maduakor and C. E. Schwartz, *Tetrahedron Lett.*, 1992, **33**, 7499–7502.
- 22 K. J. Rutan, F. J. Heldrich and L. F. Borges, *J. Org. Chem.*, 1995, **60**, 2948–2950.
- 23 B. D. Judkins, D. G. Allen, T. A. Cook, B. Evans and T. E. Sardharwala, *Synth. Commun.*, 1996, **26**, 4351–4367.
- 24 E. A. Meyer, R. K. Castellano and F. Diederich, *Angew. Chem., Int. Ed.*, 2003, **42**, 1210–1250.
- 25 (a) J. D. Dunitz and R. Taylor, *Chem. Eur. J.*, 1997, **3**, 89–98; (b) J. A. K. Howard, V. J. Hoy, D. O'Hagan and G. T. Smith, *Tetrahedron*, 1996, **52**, 12613–12622.
- 26 T. Steiner, *Angew. Chem., Int. Ed.*, 2002, **41**, 48–76.
- 27 (a) J. P. Snyder, N. S. Chandrakumar, H. Sato and D. C. Lankin, *J. Am. Chem. Soc.*, 2000, **122**, 544–545; (b) T. J. Barbarich, C. D. Rithner, S. M. Miller, O. P. Anderson and S. H. Strauss, *J. Am. Chem. Soc.*, 1999, **121**, 4280–4281.
- 28 (a) G. R. Desiraju, *Acc. Chem. Res.*, 2002, **35**, 565–573; (b) V. R. Thalladi, H.-C. Weiss, D. Bläser, R. Boese, A. Nangia and G. R. Desiraju, *J. Am. Chem. Soc.*, 1998, **120**, 8702–8710.
- 29 A. J. Mountford, D. L. Hughes and S. J. Lancaster, *Chem. Commun.*, 2003, 2148–2149.
- 30 (a) J. Parsch and J. W. Engels, *J. Am. Chem. Soc.*, 2002, **124**, 5664–5672; (b) G. M. Dubowchik, V. M. Vrudhula, B. Dasgupta, J. Ditta, T. Chen, S. Sheriff, K. Sipman, M. Witmer, J. Tredup, D. M. Vyas, T. A. Verdoorn, S. Bollini and A. Vinitzky, *Org. Lett.*, 2001, **3**, 3987–3990; (c) A. DerHovanessian, J. B. Doyon, A. Jain, P. R. Rablen and A.-M. Sapse, *Org. Lett.*, 1999, **1**, 1359–1362.
- 31 (a) E. J. Corey and T. W. Lee, *Chem. Commun.*, 2001, 1321–1329; (b) V. V. Grushin and W. J. Marshall, *Angew. Chem., Int. Ed.*, 2002, **41**, 4476–4479.

- 32 P. W. Baures, A. M. Beatty, M. Dhanasekaran, B. A. Helfrich, W. Pérez-Segarra and J. Desper, *J. Am. Chem. Soc.*, 2002, **124**, 11315–11323.
- 33 K. Nishide, Y. Hagimoto, H. Hasegawa, M. Shiro and M. Node, *Chem. Commun.*, 2001, 2394–2395.
- 34 CSD Version 5.24 of November 2002, holding over 270 000 small-molecule crystal structures. The search was limited to well-resolved (R -factor $< 7.5\%$, no disorder) neutral organic molecules, excluding metallorganic or polymeric compounds, with an intermolecular (non-bonded) distance between a C-bound F-atom and a nitrile C-atom in the range of $2.5 \text{ \AA} < d_{\text{F} \cdots \text{CN}} < 4.0 \text{ \AA}$.
- 35 W. R. Croasmun and R. M. K. Carlson (eds), *Two-Dimensional NMR Spectroscopy*, 2nd ed., VCH, Weinheim, 1994.
- 36 MedChem02 database, Daylight Chemical Information Systems, Inc., 27401, Los Altos #360, Mission Viejo, CA 92691, USA.
- 37 J. Clark and D. D. Perrin, *Q. Rev. Chem. Soc.*, 1964, **18**, 295–320.
- 38 Spartan '04 Windows, Copyright 2003, Wavefunction, Inc., 18401 Von Karman Ave., Irvine, CA 92612.
- 39 Unfavorable C–F dipole–lone pair interactions were elegantly taken in consideration to explain the primary stereoelectronic effect in the Baeyer–Villiger reaction; see: C. M. Crudden, A. C. Chen and L. A. Calhoun, *Angew. Chem., Int. Ed.*, 2000, **39**, 2852–2855.
- 40 B. A. Katz, R. Mackman, C. Luong, K. Radika, A. Martelli, P. A. Sprengeler, J. Wang, H. Chan and L. Wong, *Chem. Biol.*, 2000, **7**, 299–312.
- 41 K. Hilpert, J. Ackermann, D. W. Banner, A. Gast, K. Gubernator, P. Hadvary, L. Labler, K. Muller, G. Schmid, T. B. Tschopp and H. van de Waterbeemd, *J. Med. Chem.*, 1994, **37**, 3889–3901.
- 42 (a) L. Sebo, B. Schweizer and F. Diederich, *Helv. Chim. Acta*, 2000, **83**, 80–92; (b) T. Grawe, G. Schafer and T. Schrader, *Org. Lett.*, 2003, **5**, 1641–1644.
- 43 (a) P. R. Gerber and K. Muller, *J. Comput.-Aided Des.*, 1995, **9**, 251–268; (b) Gerber Molecular Design (<http://www.moloc.ch>).
- 44 (a) A. Albert and E. P. Serjeant, *The Determination of Ionization Constants*, T&A Constable Ltd., Edinburgh, 1971; (b) Sirius Analytical Instruments Ltd.: Applications and Theory Guide to pH-Metric pK_a and $\log P$ Determination, Revision, 1.0, August 1993; (c) Sirius Analytical Instruments Ltd.: GLp K_a instruction manual, January 1999.
- 45 A. Altomare, G. Cascarano, C. Giacovazzo, A. Guagliardi, M. Burla, G. Polidori and M. Camalli, *J. Appl. Crystallogr.*, 1994, **27**, 435.
- 46 G. M. Sheldrick, SHELX-97 program for the refinement of crystal structures, University of Gottingen, Germany, 1997.